Article:
Hackenberg, Sina orcid.org/0000-0002-2165-8827, Andrews, Stephen Joseph, Airs, R. et al. (13 more authors) (2017) Potential controls of isoprene in the surface ocean. Global Biogeochemical Cycles. GBC20531. pp. 644-662. ISSN: 0886-6236

https://doi.org/10.1002/2016GB005531

AGU PUBLICATIONS

Global Biogeochemical Cycles

RESEARCH ARTICLE
10.1002/2016GB005531

Key Points:
- Isoprene water concentrations correlated well with Chl *a*, primary production, photoprotective pigments, and cyanobacterial cell counts
- Higher isoprene concentrations relative to all respective variables were found at sea surface temperatures greater than 20°C
- Predicted isoprene water concentrations based on satellite Chl *a* compared well with observations

Supporting Information:
- Supporting Information S1

Correspondence to:
S. C. Hackenberg and L. J. Carpenter,
lucy.carpenter@york.ac.uk;
sina.hackenberg@gmail.com

Citation:
Hackenberg, S. C., et al. (2017), Potential controls of isoprene in the surface ocean, *Global Biogeochem. Cycles*, *31*, doi:10.1002/2016GB005531.

Received 18 SEP 2016
Accepted 9 MAR 2017
Accepted article online 13 MAR 2017

Potential controls of isoprene in the surface ocean

S. C. Hackenberg[1], S. J. Andrews[1], R. Airs[2], S. R. Arnold[3], H. A. Bouman[4], R. J. W. Brewin[2,5], R. J. Chance[1], D. Cummings[2], G. Dall'Olmo[2,5], A. C. Lewis[1,6], J. K. Minaeian[1], K. M. Reifel[7,8], A. Small[4], G. A. Tarran[2], G. H. Tilstone[2], and L. J. Carpenter[1]

[1]Wolfson Atmospheric Chemistry Laboratories, Department of Chemistry, University of York, York, UK, [2]Plymouth Marine Laboratory, Plymouth, UK, [3]Institute for Climate and Atmospheric Science, School of Earth and Environment, University of Leeds, Leeds, UK, [4]Department of Earth Sciences, University of Oxford, Oxford, UK, [5]National Centre for Earth Observation, Plymouth Marine Laboratory, Plymouth, UK, [6]National Centre for Atmospheric Science, University of York, York, UK, [7]Department of Botany and Plant Pathology, Oregon State University, Corvallis, Oregon, USA, [8]Now at National Biodefense Analysis and Countermeasures Center, Frederick, Maryland, USA

Abstract Isoprene surface ocean concentrations and vertical distribution, atmospheric mixing ratios, and calculated sea-to-air fluxes spanning approximately 125° of latitude (80°N–45°S) over the Arctic and Atlantic Oceans are reported. Oceanic isoprene concentrations were associated with a number of concurrently monitored biological variables including chlorophyll *a* (Chl *a*), photoprotective pigments, integrated primary production (intPP), and cyanobacterial cell counts, with higher isoprene concentrations relative to all respective variables found at sea surface temperatures greater than 20°C. The correlation between isoprene and the sum of photoprotective carotenoids, which is reported here for the first time, was the most consistent across all cruises. Parameterizations based on linear regression analyses of these relationships perform well for Arctic and Atlantic data, producing a better fit to observations than an existing Chl *a*-based parameterization. Global extrapolation of isoprene surface water concentrations using satellite-derived Chl *a* and intPP reproduced general trends in the in situ data and absolute values within a factor of 2 between 60% and 85%, depending on the data set and algorithm used.

1. Introduction

Biogenic volatile organic compounds have profound impacts on atmospheric chemistry, predominantly by forming tropospheric ozone, modifying the oxidative capacity of the atmosphere, and contributing to secondary organic aerosol [e.g., *Carlton et al.*, 2009; *Claeys et al.*, 2004]. Isoprene, emitted mainly from trees and plants, accounts for around half of the global biogenic nonmethane hydrocarbon emissions, with an estimated terrestrial source strength of 500 Tg C yr^{-1} [*Guenther et al.*, 2012]. More recent research has suggested that an oceanic source of isoprene could significantly impact atmospheric chemistry and cloud microphysical properties in the remote marine boundary layer, despite its much lower emission strength in this region [*Meskhidze and Nenes*, 2006; *Wingenter et al.*, 2007; *Gantt et al.*, 2009; *Arnold et al.*, 2009; *Metzger et al.*, 2010]. However, estimates of global oceanic emissions vary by up to 2 orders of magnitude between bottom-up (seawater derived; ~0.1–1 Tg C yr^{-1}) [*Arnold et al.*, 2009; *Luo and Yu*, 2010; *Palmer and Shaw*, 2005; *Ito and Kawamiya*, 2010; *Gantt et al.*, 2009] and top-down approaches (1.68–11.6 Tg C yr^{-1}) [*Arnold et al.*, 2009; *Luo and Yu*, 2010]. The factors controlling marine isoprene emissions are still poorly understood, partly due to a paucity of field measurements, especially those with suitable supporting data.

A review of previous work on marine isoprene and its likely oceanic controls can be found in *Shaw et al.* [2010], which is briefly repeated and extended here with more recent studies. *Bonsang et al.* [1992] reported the first observations of isoprene in seawater and suggested a biological source based on the association with concurrently measured chlorophyll *a* concentrations ([Chl *a*]). This was further supported by a number of field measurements [*Milne et al.*, 1995; *Broadgate et al.*, 1997; *Baker et al.*, 2000; *Wingenter et al.*, 2004; *Moore and Wang*, 2006; *Kurihara et al.*, 2010, 2012; *Tran et al.*, 2013; *Kameyama et al.*, 2014; *Zindler et al.*, 2014; *Ooki et al.*, 2015] and laboratory studies [*Moore et al.*, 1994; *McKay et al.*, 1996; *Shaw*, 2001; *Shaw et al.*, 2003; *Gantt et al.*, 2009; *Bonsang et al.*, 2010; *Exton et al.*, 2013] that observed correlations with Chl *a*. Additionally, photochemical production from the sea surface microlayer has recently been proposed as a potential abiotic source [*Ciuraru et al.*, 2015].

The importance or precise nature of a biological sink within the ocean is still unconfirmed. *Acuña Alvarez et al*. [2009] reported isoprene consumption by various hydrocarbon-degrading bacteria from estuarine sediments in laboratory experiments, while *Shaw et al*. [2003] did not find an effect of introducing bacteria into cultures.

Based on these observations of isoprene-Chl *a* relationships, along with Chl *a*-normalized laboratory monoculture production rates, several authors have attempted a global extrapolation of isoprene fluxes. *Palmer and Shaw* [2005] assumed steady state oceanic isoprene concentrations, scaling isoprene production by satellite [Chl *a*] and balancing it with losses due to chemical and biological removal, water column mixing, and air-sea exchange (the latter being the largest loss term by far). They then used the obtained isoprene water concentrations to model global fluxes. *Arnold et al*. [2009] refined this approach by differentiating isoprene production rates by phytoplankton functional type (PFT), following findings from laboratory studies. Production in the water column and loss to the atmosphere were taken to be in steady state, and both remotely sensed [Chl *a*] and PFT data based on the PHYSAT algorithm were used for global scaling.

Another recent global emission estimate has been computed using a physically-based method that takes into account known influences of several additional parameters on isoprene production based on laboratory studies [*Gantt et al*., 2009]. It uses global PFT distributions and [Chl *a*] from satellite data with PFT-specific production rates and ambient light levels to derive hourly production within the entire euphotic depth of the water column. As in the previous methods, the production is assumed to result in instantaneous emission to the atmosphere, which in combination with the light dependence in this approach leads to a diurnal profile of the flux. However, observations suggest that significant isoprene production takes place at depths of 5 m or deeper [cf. *Bonsang et al*., 1992; *Milne et al*., 1995; *Moore and Wang*, 2006; *Tran et al*., 2013] (vertical distributions in this work) and so would only gradually be vented to the atmosphere, which would smooth out the diurnal nature of production. In their paper, Gantt and coworkers already reported that field observations [*Matsunaga et al*., 2002] did not show the strong diurnal pattern and zero nighttime emissions that their model predicted.

Despite a qualitative consensus about the existence of a biological control, published equations to predict isoprene concentrations in water, based on [Chl *a*] vary widely (this is discussed further in section 3.4 and Table 4). Likely reasons are the apparent dependence of isoprene production on PFTs, or even lower taxonomic groups, as well as growth conditions in laboratory cultures [*Shaw et al*., 2003; *Gantt et al*., 2009; *Bonsang et al*., 2010; *Exton et al*., 2013], and also variations observed in the field with sea surface temperature (SST) [*Ooki et al*., 2015].

This work reports a substantial number of new isoprene observations in the surface ocean and marine atmosphere across a large range of latitudes, thereby significantly increasing the available data set and enabling the estimation of sea-to-air fluxes. Supporting measurements of the proposed and potential additional controls provide new field data to improve our understanding of the different parameters influencing marine isoprene. We investigate the suitability of several parameterizations, derived from the new data, for predicting isoprene fluxes on a global scale.

2. Experimental

2.1. Cruise and Sampling Overview

Sampling took place during the AMT 22 cruise (Atlantic Meridional Transect, UK-South Atlantic, October/November 2012, RRS *James Cook*), AMT 23 cruise (UK-South Atlantic, October/November 2013, RRS *James Clark Ross* (JCR)), ACCACIA 1 cruise (March 2013, Arctic, R/V *Lance*), and ACCACIA 2 cruise (JR288, Arctic, July/August 2013, JCR). Cruise tracks are indicated in Figure 1 and Figure S1 (supporting information).

CTD (conductivity-temperature-depth) casts were performed twice daily (pre-dawn and solar noon) during AMT 22 and 23 and once daily (morning) during ACCACIA 1 and 2. Water was subsampled from the Niskin bottles (20 L) for further processing, described in detail separately for each variable. Various measurements were also made from the ships' clean underway seawater supply inlet (nominal depth 5–6 m).

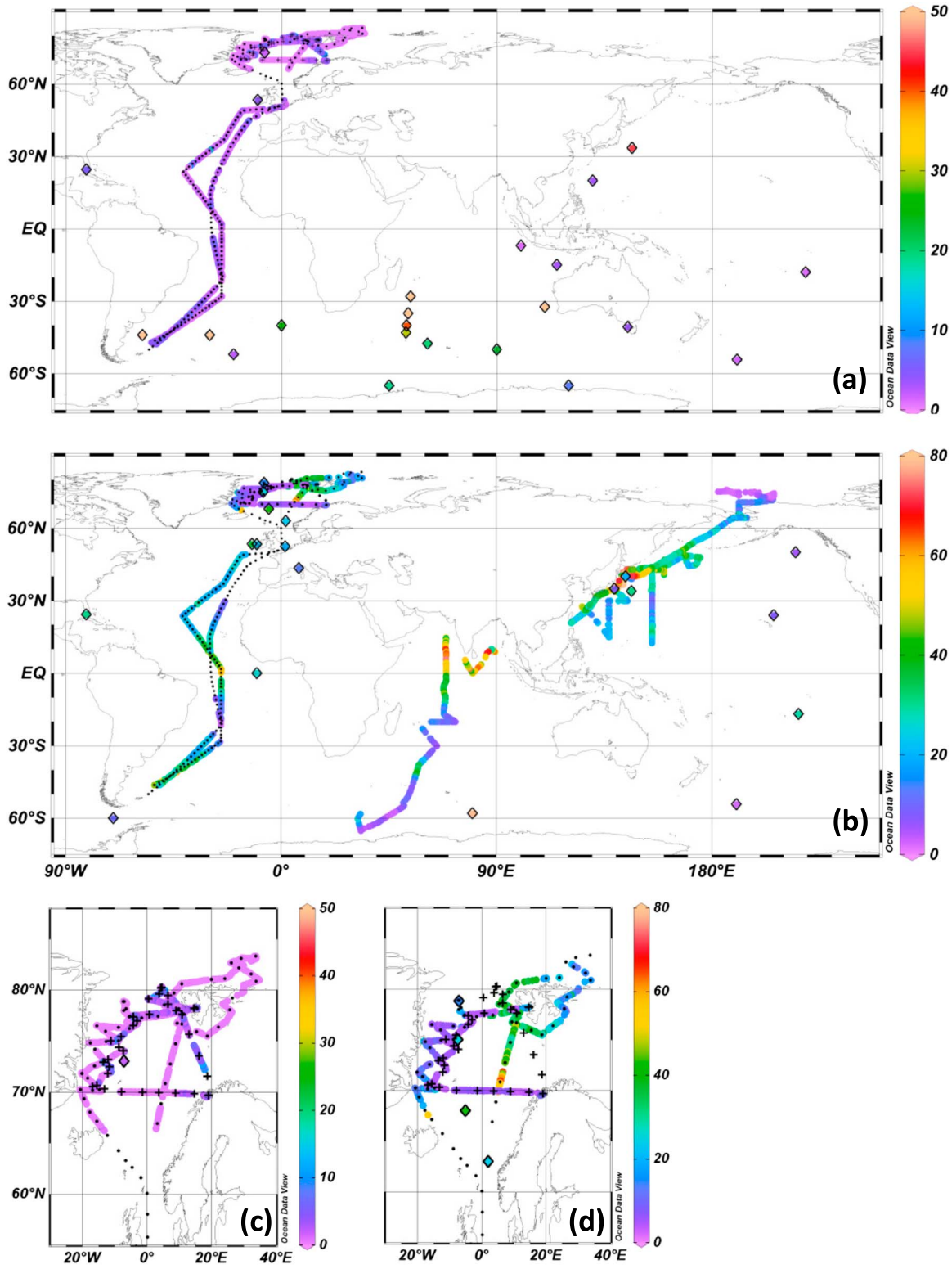

Figure 1. (a) Isoprene air mixing ratios (including data < DL as 0.5 × DL; pptv) and (b) isoprene concentration in the surface ocean (pmol L^{-1}) along the cruise tracks (dotted black lines; also see Figure S1) for AMT 22 and 23 and ACCACIA 1 and 2. (c) Air and (d) water data in enlarged ACCACIA sampling region (plus signs for ACCACIA 1). Also shown are published values for the Pacific, Indian, and Southern Oceans taken from *Ooki et al.* [2015] and further air and water concentrations from the literature which are also listed in Table 2 (large colored diamonds). Measurements shown from oceanic sites only, no remotely sensed or coastal data. Literature values shown are best estimates of averages and locations from graphs or tables; several points are shown per study where data sets covered larger areas. Plots created with Ocean Data View [*Schlitzer*, 2016].

2.2. Isoprene Measurements by (autoP&T)-TD-GC-MS

Trace gases were measured in water and air during all four cruises by (automated Purge & Trap)-Thermal Desorption-Gas Chromatography-Mass Spectrometry ((autoP&T)-TD-GC-MS), with details given in the supporting information (Text S1).

Briefly, isoprene in air was measured as discrete samples of 1–2 L air, from a continuously pumped air inlet. Isoprene in seawater was analyzed from the ships' pumped nontoxic seawater supplies as well as from CTD casts from within the photic depth, using the semiautomated P&T system described in *Andrews et al*. [2015], with modifications detailed in the supporting information. Analysis was performed by GC-MS, with regular calibrations using a premixed gas standard. Detection limits were calculated dynamically to account for changing instrument sensitivity and ranged between 0.1–5 pmol L^{-1} and 0.1–2.5 pptv (parts per trillion) for water and air, respectively, and the uncertainty of the analysis was typically around 10–20%. Air data were filtered for contamination arising from the ship's exhaust using hydrocarbon concentration thresholds.

2.3. Biological and Supporting Data

With the exception of ACCACIA 1, a variety of biological data sets were collected and analyzed during the cruises, with methods described in the supporting information (Text S2). Data included gross biomass (Chl *a*) and integrated primary production (intPP) using the methods described in *Tilstone et al.* [2009], as well as flow cytometry and pigment data from high-performance liquid chromatography analysis (HPLC). Furthermore, CHEMTAX analysis was performed for ACCACIA 2 pigment data.

Meteorological data such as wind speed and sea surface temperature (SST) were obtained from the ship systems, provided by the British Oceanographic Data Centre (BODC).

2.4. Further Analysis

The isoprene sea-to-air flux was calculated following the approach of *Johnson* [2010], assuming air concentrations of zero due to the large degree of supersaturation of the gas in seawater (see supporting information Text S3.1). [Chl *a*] and SST were extracted from Moderate Resolution Imaging Spectroradiometer (MODIS)-Aqua (http://oceancolor.gsfc.nasa.gov/cms/); intPP was calculated using MODIS-Aqua Chl *a* and photosynthetically active radiation (PAR) and mixed layer depth from a climatology (see supporting information Text S3.2). Isoprene concentrations were produced from the satellite data using the SST-binned combined regressions (ALL) detailed in section 3.3 for [Chl *a*] and $intPP_{(total)}$.

3. Results and Discussion

3.1. Isoprene Air and Water Concentrations

A comprehensive, internally consistent set of isoprene atmospheric mixing ratios and surface ocean concentrations is reported here, spanning around 125° of latitude in the Atlantic and Arctic Oceans at comparatively high spatial and temporal resolution. The data substantially increase the number of currently published marine isoprene measurements, especially in oligotrophic oceanic regions [cf. *Shaw et al*., 2010], as can be seen in Figure 1.

In a typical depth profile (Figure 2), the isoprene concentrations generally followed the shape of the Chl *a* profile, with the maximum isoprene concentration slightly shallower than the deep chlorophyll maximum when present. This is in agreement with published vertical distributions [*Bonsang et al*., 1992; *Milne et al*., 1995; *Moore and Wang*, 2006; *Tran et al*., 2013].

As shown in Figure and summarized in Table 1, surface ocean isoprene concentrations varied between 1 and 66 pmol L^{-1}, with mean concentrations around 20 pmol L^{-1} for all cruises except the Arctic winter/spring cruise, during which concentrations were much lower (mean of 4 pmol L^{-1}). This compares well with previously published mean values of typically 25–30 pmol L^{-1} in the Atlantic and around 10–80 pmol L^{-1} across all oceans (Table 2). Some authors have also observed much higher concentrations, mostly where biological productivity in the study region was high (e.g., coastal or spring blooms) [*Tran et al*., 2013; *Kameyama et al*., 2014; *Ooki et al*., 2015].

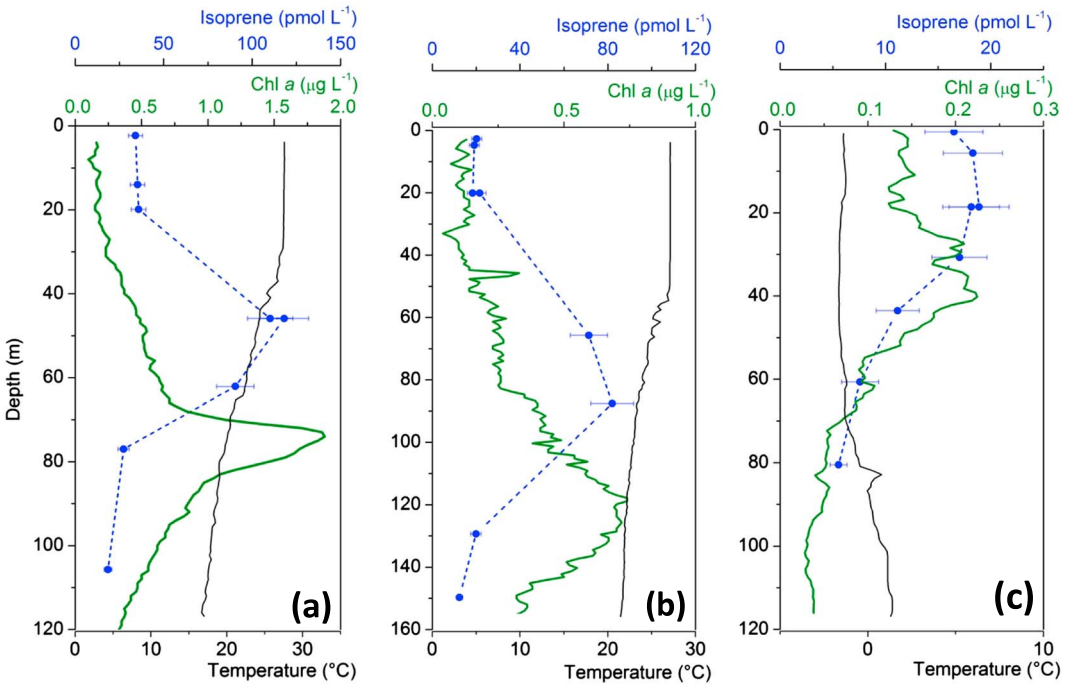

Figure 2. Typical isoprene (blue) depth profiles alongside CTD fluorescence sensor Chl *a* (green) and temperature (black) traces to indicate biological activity and mixed layer depth; (a) tropical North Atlantic, 14°N, 34°W (CTD 30, AMT 22); (b) North Atlantic Gyre, 23°N, 41°W (CTD 23, AMT 22); and (c) Arctic, 83°N, 26°E (CTD 18a, ACCACIA 2). Error bars for isoprene data represent the measurement uncertainty. Further depth profiles available in the full data set held at BODC.

There was no significant difference between average daytime and nighttime concentrations during any of the cruises (Figure 3), suggesting a lack of diurnal variation for isoprene in surface waters. (Day defined using a threshold of modeled $jNO_2 > 5 \times 10^{-5}\ s^{-1}$ (GEOS-Chem v9.2, 4 × 5° resolution) [*Sherwen et al.*, 2016] during the sampling period, as the photolysis rate of NO_2 (jNO_2) is zero at night, threshold allowing for noise in the data.) There were too few ACCACIA 2 nighttime values (due to light summer nights) to establish a meaningful difference to daytime.

Atmospheric mixing ratios were consistently low and often below the detection limit (DL), with mean values of around 1–3 pptv. This lies at the lower end of the range of previous observations; several studies found tens to a couple of hundreds of pptv isoprene above phytoplankton blooms or in coastal areas (Table 2).

Table 1. Isoprene Concentrations in Water and Air for Each of the Four Cruises Reported in This Study[a]

	Cruise[b]	Mean (Range)	Mean (0.5 × DL)	Median (*n*)	Median (*n*) (0.5 × DL)	DL Range[d]	Surface CTD[e] Mean (*n*)
Air (pptv)	AMT 22	1.88 (<DL–18.28)	1.47	1.51 (*347*)	1.07 (*496*)	0.09–2.42	
	AMT 23[c]	2.76 (<DL–10.24)	2.72	2.27 (*502*)	2.24 (*509*)	0.05–0.47	
	ACCACIA 1[c]	3.37 (<DL–13.82)	3.17	2.61 (*610*)	2.41 (*648*)	0.03–0.27	
	ACCACIA 2	0.41 (<DL–1.61)	0.19	0.35 (*150*)	0.16 (*891*)	0.08–0.71	
Water (pmol L^{-1})	AMT 22	26.76 (8.75–63.36)	-	23.18 (*290*)	-	0.12–2.57	29.59 (*37*)
	AMT 23	18.74 (1.12–38.20)	-	17.20 (*196*)	-	0.07–0.12	25.85 (*28*)
	ACCACIA 1	4.40 (1.96–10.57)	-	4.25 (*166*)	-	0.28–0.68	6.29 (*9*)
	ACCACIA 2	24.12 (3.86–66.38)	-	19.91 (*221*)	-	0.80–4.88	22.01 (*43*)

[a]Mean and median are given for only data > DL as well as for all data, substituting a value of half the DL (0.5 × DL) for points that fall below the DL but are otherwise not flagged as bad (or probably bad) data. A dash indicates that no data were < DL. Number of data points *n* applies to both mean and median (only shown with median).
[b]AMT cruises: North and South Atlantic (October/November); ACCACIA 1: Arctic (March); and ACCACIA 2: Arctic (July/August).
[c]May be compromised due to hydrocarbon contamination.
[d]Dynamic DL.
[e]Surface CTD (<10 m depth).

Table 2. Published Air and Water Concentrations of Isoprene

Mean ± Standard Deviation (Range)	[Notes]	Location[a] (Month)	Reference
		Air (*pptv*)	
<2–36		South Pacific (May/Jun);	*Bonsang et al.* [1992]
<10–20		Southern Indian Ocean (all year)	
<5–11		Florida Gulf (Sep)	*Milne et al.* [1995]
3.9; 6.2 (<5–24)	[NW; SW winds]	Mace Head Observatory (Aug)	*Lewis et al.* [1997]
2.6	[NW; SW winds]	Mace Head Observatory (Aug)	*Lewis et al.* [1999]
<0.1–250		SE Asian Sea, Indian Ocean, SO (two cruises, Nov–Mar)	*Yokouchi et al.* [1999]
<1.6; 5.7	[night; day]	Cape Grim Observatory (summer)	*Lewis et al.* [2001]
45 (7.2–110)		Western North Pacific (May)	*Matsunaga et al.* [2002]
1.9; 0.9	[oceanic; arctic air]	Arctic (summer)	*Hopkins et al.* [2002]
<3		Southern Ocean (Jan)	*Wingenter et al.* [2004]
180 (<60–2380)		Mesocosm (Norway; Jun)	*Sinha et al.* [2007]
67 ± 40 and 73 ± 27[c]	[remote]	Southern Ocean (Jan)	*Williams et al.* [2010]
274 ± 40 and 203 ± 32[c]	[bloom]		[leg 1]
2.1 ± 2.1[c]	[remote]	Southern Ocean (Jan/Mar)	*Williams et al.* [2010] (average of both legs)
26 (<(1–5) − 48)	[remote]	Southern Ocean (Jan)	*Yassaa et al.* [2008]
99 (60–138)	[distant bloom]		[leg 1][g]
187 (32–375)	[bloom]		
40 (20–340)	[south of 35°S]	Southern Indian Ocean (Dec)	*Colomb et al.* [2009]
20 ± 20	[background]		
14	[2006]	Cape Grim observatory	*Lawson et al.* [2011]
21	[2007]	(hourly mean, marine air)	and *Galbally et al.* [2007]
14		SW Pacific Ocean (Mar)	*Lawson et al.* [2015]
		Water (*pmol* L^{-1})	
Up to 23.3		Mediterranean (Oct/May)	*Bonsang et al.* [1992]
Up to 41		and Pacific (Apr/May/Jun)[d]	
30.8 ± 16.3 (9.8–50.8)		Florida Gulf (Sep)	*Milne et al.* [1995]
0.7–54		North Sea (Feb–Sep)	*Broadgate et al.* [1997]
14–61		Eastern Atlantic (May)	*Baker et al.* [2000]
30 (<12–94)		Western North Pacific (May)	*Matsunaga et al.* [2002]
1.8	[out of patch]	Southern Ocean (Jan)	*Wingenter et al.* [2004]
7.3	[in patch]		
20.8	[3 km off coast]	Mace Head Observatory (Sep)	*Broadgate et al.* [2004]
19.7 (3.8–68.2)		Western North Pacific (Apr)	*Kurihara et al.* [2010]
70.6 ± 17.3		NW Pacific (Jul–Aug)	*Kameyama et al.* [2010][e]
7.3 (4.4–10.0)		Sagami Bay (Japan/Pacific; Apr–Dec)	*Kurihara et al.* [2012]
26 ± 31 (1–541)		Arctic and Atlantic Oceans (Jun/Jul)	*Tran et al.* [2013]
78.7 (0.2–348)		Southern Ocean (Dec–Jan)	*Kameyama et al.* [2014]
25.7 ± 14.7 (~5–60)		East Atlantic (Nov)	*Zindler et al.* [2014]
27 (1.3–121)	[basin][f]	Arctic, Pacific, Indian,	*Ooki et al.* [2015]
44 (1.5–165)	[slope][f]	and Southern Oceans	
30 (2.7–136)	[shelf][f]		

[a] Ship unless specified.
[b] Programmable temperature vaporization-GC-FID.
[c] Median ± median absolute deviation.
[d] Open ocean only.
[e] Values also reported as part of *Ooki et al.* [2015] data set.
[f] Basin (bottom depth >2000 m), slope (200–2000 m), and shelf (<200 m) areas.
[g] Same cruise as *Williams et al.* [2010] but unclear whether same samples.

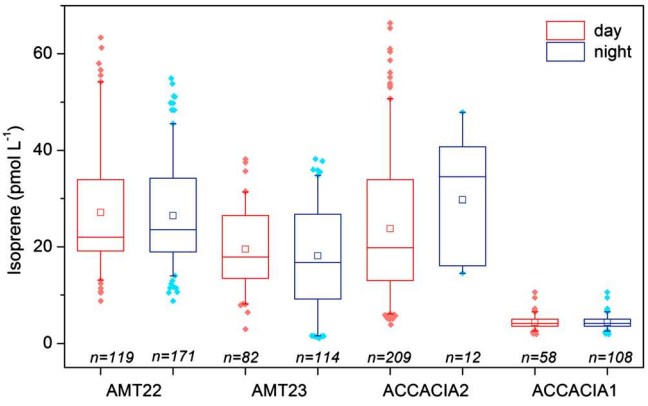

Figure 3. Daytime (red) and nighttime (blue) isoprene concentrations in water for all four cruises; day defined as model $jNO_2 > 5 \times 10^{-5}\ s^{-1}$; for details, see main text. Mean (open square), median (line), 25th–75th percentiles (box); 5th–95th percentiles (whiskers), and outlier data points (filled diamonds).

The magnitude of our reported atmospheric concentrations is consistent with past studies in which an insignificant role for isoprene for marine secondary organic aerosol has been inferred [*Arnold et al*., 2009]. Our air measurements also provided a constraint for flux calculations in this work (see Text S3.1). Similar to water, no diurnal trends were observed in air, even when levels were consistently above the detection limit. However, the generally low biological activity during our cruises is comparable to "background" or "remote" regions for which isoprene near or below the detection limit is often reported (Table 2). Careful filtering for potential ship influence in this work may also have resulted in lower values; comparisons are limited as the extent of filtering has, to our knowledge, not been described in detail for other studies.

As a substantial part of our air data fell below the DL, mean and median values were also calculated including a value of 0.5 × DL for data < DL. The results should represent a more accurate approximation of the typical isoprene mixing ratios by accounting for low values (and assuming that samples < DL are unlikely to be at zero). A mean or median calculated from only data > DL is necessarily biased toward higher values and omits some of the valid data (cf. Table 1).

3.2. Sea-to-Air Fluxes

Fluxes determined in this study are of comparable magnitude to previously published fluxes for the Atlantic and Arctic Oceans (Figure 4 and values in Table S1, supporting information), taking into account the overall large spatial and temporal variability. The error bars shown on the previously published fluxes reflect the large range in isoprene concentrations observed within each study, with an additional distinction between different water masses in the *Tran et al*. [2013] data. The *Tran et al*. [2013] data shown are the two water masses with the lowest and highest isoprene concentrations and fluxes observed during that study, to highlight the extent of the variation in the North Atlantic and Arctic Oceans.

There is a further distinction for different approaches to the flux calculations in two studies (values in Table S1). The calculated isoprene fluxes from *Meskhidze and Nenes* [2006] highlight that the choice of empirical relationship strongly influences results from remotely sensed Chl *a*: mean fluxes calculated according to *Palmer and Shaw* [2005] (based on laboratory production rates) were 3 times higher than the SOFeX method (calculated from in situ Southern Ocean isoprene concentrations), even though both approaches scaled surface isoprene by the same satellite [Chl *a*]. Furthermore, the choice of flux calculation can affect the results by more than 50%, as evident from the two methods employed by *Tran et al*. [2013]. Owing to this combination of large variations in concentrations and calculations, it is difficult to obtain close agreement between different studies. Considering this, the mean values and ranges for the cruises from this work generally compare very well (within a factor of 2) with the corresponding literature, such as Atlantic values from various studies, or the in-ice ACCACIA 2 and all ACCACIA 1 data with *Tran et al*. [2013] polar waters.

From equation (1) (supporting information Text S3.1), it can be seen that the main controls of the calculated bottom-up fluxes are wind speed and isoprene surface ocean concentration, as k_w is strongly dependent on wind speed and flux scales linearly with seawater concentration. The former is most obvious in Figure 4 for

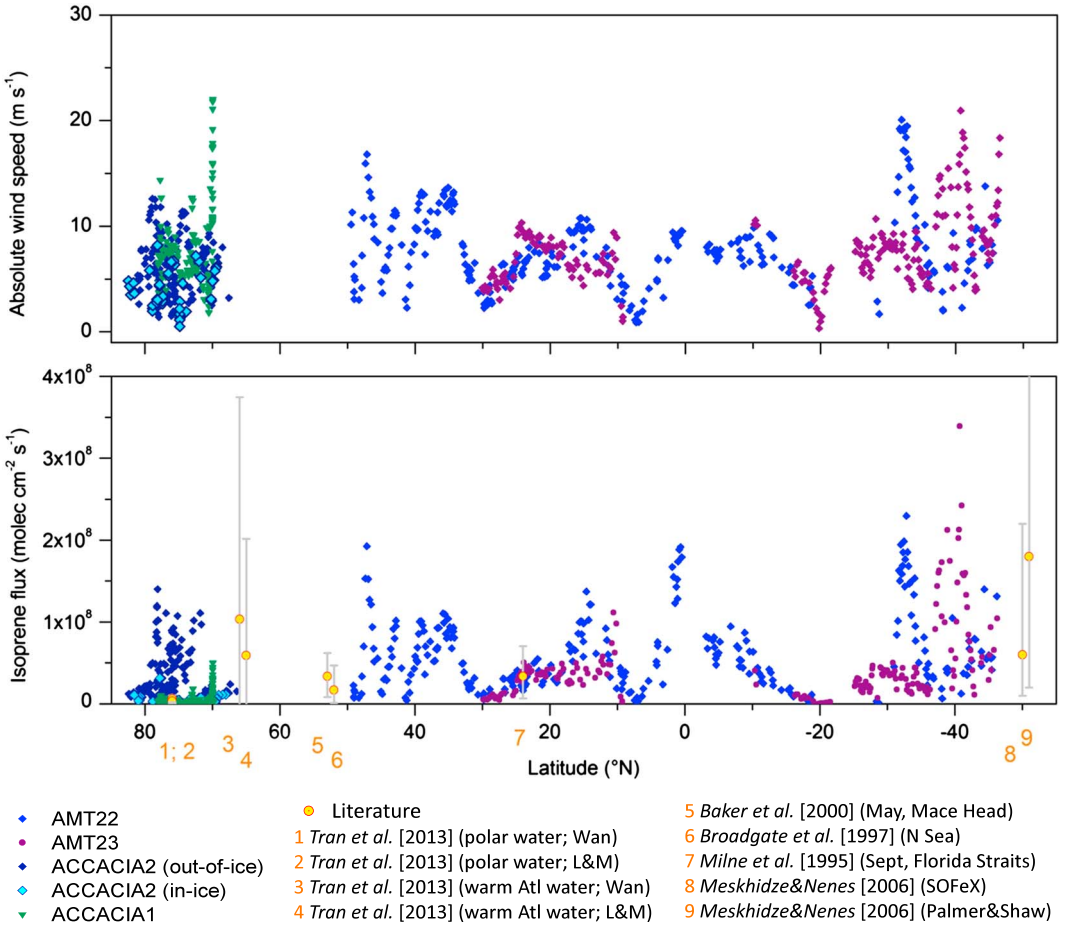

Figure 4. Latitudinal transect of seawater-derived sea-to-air fluxes for all four cruises alongside wind speed (at ~20 m above sea level) and literature values for Atlantic waters, with ACCACIA 2 (>60°N only) separated into in-ice and out-of-ice sampling regions. Literature values shown at approximate latitudes with error bars representing ranges given in the references; Wan/L&M = flux parameterization from *Wanninkhof* [1992] and *Liss and Merlivat* [1986], respectively; for *Meskhidze and Nenes* [2006], see main text.

the AMT cruises, with distinctly higher fluxes for the periods with higher wind in one year compared to the other year (around 30–45°S), while isoprene concentrations matched closely between both years (see Figure 1a).

The latter is evident from the larger isoprene concentrations for ACCACIA 2 out-of-ice compared to in-ice, with higher fluxes despite similar wind speeds. As wind speed can be obtained on a global scale from a number of sources including climatologies, comprehensive databases, and satellite products (e.g., from http://giovanni.gsfc.nasa.gov/giovanni/), a better understanding of the factors affecting isoprene concentrations would be a large step toward a more accurate global extrapolation of isoprene fluxes. We will therefore now focus on potential controls of isoprene in the surface water.

3.3. Potential Biological Controls on Seawater Isoprene Concentrations

Based on previously published associations of marine isoprene with phytoplankton biomass (Chl *a*), PFTs, and general biological productivity, relationships of surface ocean isoprene concentrations with concurrently monitored biological variables were investigated. Spatial and temporal variation of selected biological variables is shown alongside isoprene concentrations in Figure 5. These analyses were not possible for ACCACIA 1 due to the lack of supporting biological data; therefore, the cruise was excluded from the following investigations. Due to the nature of the cruise tracks, AMT cruises are shown as latitudinal transects, while ACCACIA data are shown as time series.

In order to explore controls on concentrations of isoprene in seawater, we assume that concentrations are directly correlated with production rates, i.e., that oceanic losses do not vary significantly across the

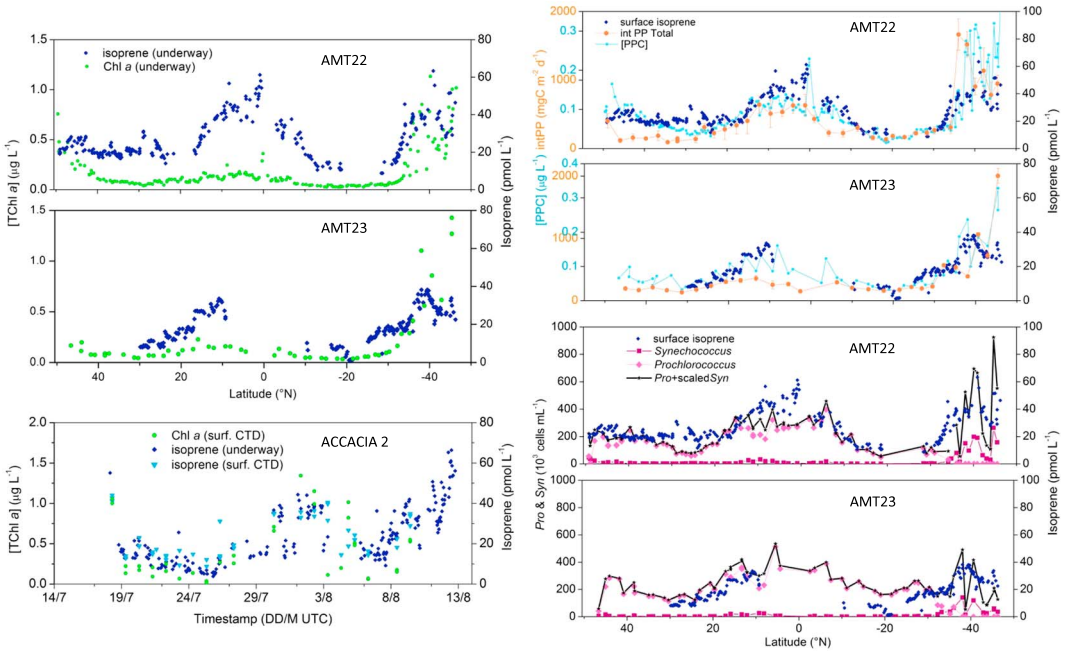

Figure 5. Transect/time series plots of surface ocean isoprene concentrations alongside selected biological measurements: total Chl *a*, sum of photoprotective carotenoids (PPC; sum of aeaxanthin, alloxanthin, diadinoxanthin, α- and β-Carotenes, and diatoxanthin), integrated primary production (intPP total), and *Synechococcus* and *Prochlorococcus* cell counts (*Syn*, *Pro*; *Syn* in *Syn* + *Pro* are scaled by a factor of 3.5 to account for cell-normalized isoprene production rates given in *Shaw et al*. [2003]).

different water bodies sampled. Chemical and physical loss rates due to reaction in the water column and downward mixing are believed to be slow, with estimated lifetimes of 19, >1000, and >250 days with respect to reaction with OH, singlet oxygen, and losses due to mixing, respectively [*Palmer and Shaw*, 2005]; thus, to a first approximation they can be assumed to be constant. (Using the values of $k_{1O2} = 10^6\,M^{-1}\,s^{-1}$ and $[^1O_2] = 10^{-14}\,M$ cited in *Palmer and Shaw* [2005] results in a calculated lifetime of 1150 rather than 115 days as stated by the authors. Using the value of $k_{1O2} = 3.7 \times 10^4\,M^{-1}\,s^{-1}$ (in chloroform solution) given in the original reference [*Monroe*, 1981], the lifetime with respect to singlet oxygen becomes >30 000 days.) Biological losses as a result of bacterial consumption were similarly assumed to be very small by these authors, based on evidence from laboratory experiments by *Shaw et al*. [2003]. The main loss from the surface ocean is, in fact, due to sea-air gas exchange, which is strongly dependent on wind speed (see section 3.2 above). This means that our assumption breaks down at high wind speeds especially, as the concentrations are controlled by losses to a larger extent and therefore no longer proportional to production (also observed by *Moore and Wang* [2006] outside a fertilized patch).

Several core measurements are collected on AMT voyages each year, including pigments, primary production (PP), and phytoplankton abundance and community composition. Typical results are described in detail in *Robinson et al*. [2002], *Tilstone et al*. [2009, 2015a, 2015b], *Tarran et al*. [2006], *Heywood et al*. [2006], and *Aiken et al*. [2009]. Significant linear relationships were found (for each cruise and for combined data sets) between isoprene and Chl *a*, other pigments including the sum of photoprotective carotenoids (PPC), some PFTs, and PP (only AMT data for the latter two). Correlations generally improved when binned by sea surface temperature (SST) with a threshold of 20°C (Table 3 and Figure 6). The threshold value was chosen based on inspection of the correlation plots for each variable, which generally exhibited a change in slope at that value (Figure 6; also cf. Figures S2–S5 in the supporting information). For variables where binning produced an insignificant correlation ($p > 0.05$) for at least one bin, only relationships for the complete data set are shown and used for further calculations.

Regression equations were calculated as the Robust Line of Organic Correlation (RLOC), which is affected less than the LOC approach by outliers and points below the detection limit [*Khalil and Adamowksi*, 2012]. Equations were determined for each data set internally (A22 for AMT 22, A23 for AMT 23, and Ac2 for

Table 3. Summary of Linear Relationships Between Isoprene and the Variables With the Most Consistent Correlations for All Three Cruises, As Well As the Entire Data Set (ALL), Binned by SST Where a Significant Correlation ($p < 0.05$) Existed for Both Bins

Parameter	SST/°C	Cruise (*n*)	Regression Equation	R^2
Chl *a* (by HPLC)	*<20*	AMT 22 (*39*)	37.9*[Chl *a*] + 17.5	0.37
		AMT 23 (*11*)	15.1*[Chl *a*] + 18.4	0.55
		ACCACIA 2 (*34*)	34.1*[Chl *a*] + 11.1	0.61
		ALL (*84*)	33.2*[Chl *a*] + 13.7	0.33
	≥20	AMT 22 (*93*)	300*[Chl *a*] − 3.35	0.60
		AMT 23 (*22*)	103*[Chl *a*] + 5.58	0.82
		ALL (*115*)	266*[Chl *a*] − 1.68	0.54
Photoprotective carotenoids (PPC)	*<20*	AMT 22 (*39*)	97.6*[PPC] + 19.5	0.50
		AMT 23 (*11*)	87.3*[PPC] + 12.9	0.33 ($p = 0.06$)
		ACCACIA 2 (*34*)	155*[PPC] + 6.59	0.47
		ALL (*84*)	102*[PPC] + 14.4	0.48
	≥20	AMT 22 (*93*)	377*[PPC] − 1.88	0.66
		AMT 23 (*22*)	176*[PPC] + 2.75	0.68
		ALL (*115*)	345*[PPC] − 0.81	0.61
Pro + *Syn* (scaled *Syn*) (AMT only)	*<20*	AMT 22 (*19*)	4.70×10^{-5}*[*Pro* + *Syn*] + 20.0	0.53
		ALL (*32*)	7.07×10^{-5}*[*Pro* + *Syn*] + 13.5	0.45
	≥20	AMT 22 (*44*)	8.49×10^{-5}*[*Pro* + *Syn*] + 5.75	0.56
		ALL (*66*)	8.97×10^{-5}*[*Pro* + *Syn*] + 9.23	0.34
	all data [a]	AMT 23 (*34*)	1.36×10^{-5}*[*Pro* + *Syn*] − 11.2	0.12
$intPP_{Total}$ (AMT only)	*<20*	AMT 22 (*10*)	0.017*(intPP) + 19	0.64
		ALL (*16*)	0.017*(intPP) + 16	0.30
	≥20	AMT 22 (*21*)	0.059*(intPP) + 8.2	0.73
		ALL (*32*)	0.086*(intPP) + 0.084	0.67
	all data [a]	AMT 23 (*17*)	0.051*(intPP) + 1.4	0.32

[a]Relationship insignificant for lower SST ($p > 0.4$), so only nonbinned results are shown. Regressions calculated using [isoprene] in pmol L^{-1}, [TChl *a*] and [PPC] in μg L^{-1}, [*Pro* + *Syn*] in cells mL^{-1}, and (intPP) in mg C m^{-2} d^{-1}. Abbreviations see Figure 5. PPC; see Figure 6.

ACCACIA 2) and also for all available data sets for that variable combined (ALL; may refer to all three cruises or only AMT data; Table 3).

3.4. Isoprene-Pigment Relationships

Slopes of the isoprene-Chl *a* correlations for waters with SST <20°C in the current study (Table 3) are of the same order of magnitude as in published relationships for similarly low-SST regions, listed in Table 4. The threshold SST of around 20°C for these relationships agrees in principle with findings by *Ooki et al*. [2015] who calculated different linear regressions for different SST bins. Their data were, however, divided into four SST bins (<3.3, 3.3–17, 17–27, and >27°C) as opposed to only two in this work (see section 3.3). It is likely that the SST is an indicator of changes in biological variables rather than a direct cause of the change in isoprene emissions. The differences between *Ooki et al*. [2015] and our work (cf. Figure 7) could stem from differences in the phytoplankton community between the Atlantic and Pacific/Indian Oceans, different sampling seasons, and frequencies and different [Chl *a*] measurement techniques (see below). The discrepancies between the studies indicate that either data set is likely not directly applicable to all parts of the world's oceans and further refinement is needed in order to obtain a more accurate global algorithm, especially for Arctic regions.

Exton et al. [2013] also reported different isoprene production rates (normalized to [Chl *a*]) from phytoplankton monocultures grown at different temperatures in accordance with their origins (polar, temperate, or tropical). However, the relative difference in slope between the temperate and tropical regimes was considerably smaller than between slopes for low- and high SST isoprene-[Chl *a*] correlations in the current study (factors of <2 and 6–8, respectively, even larger for *Ooki et al*. [2015]; Table 4), which could point to limited comparability of laboratory and field data. This might include additional controls on the production in the field such as the proposed photochemical surface source [*Ciuraru et al*., 2015] and/or currently unknown loss processes. It highlights that global emission estimates based on laboratory data

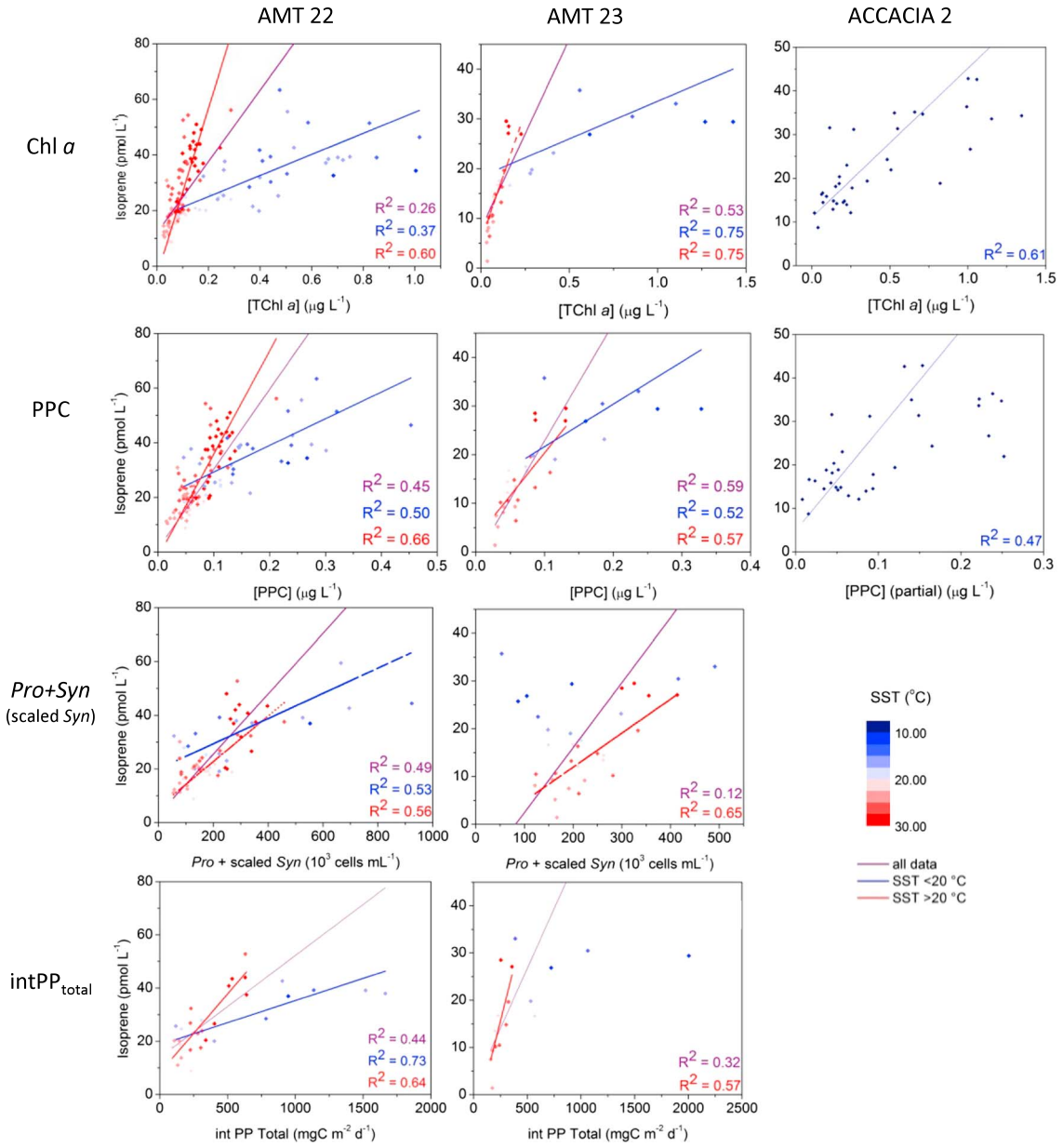

Figure 6. Correlations of isoprene with several biological variables (Chl *a*, PPC, *Pro* + *Syn*, and $intPP_{Total}$) for AMT 22, AMT 23, and ACCACIA 2. Colored by SST and binned for regression analysis (threshold 20°C); regression lines and R^2 values only shown for significant correlations ($p < 0.05$). For abbreviations, see Figure 5; Diato for PPC not available for ACCACIA 2.

may not accurately reflect those in the wider marine environment and validation against field measurements is required.

A significant limitation to comparability between studies, unrelated to potential differences in isoprene measurements, may be Chl *a* measurement techniques. HPLC pigment analysis can be considered the most accurate method but is more expensive and labor intensive than fluorometric Chl *a* analysis. The latter is faster and easier, allowing shipboard analysis to be completed typically in less than 2 days (including 24 h for pigment extraction). The different techniques can provide results that vary by up to a factor of 2, with HPLC Chl *a* concentrations typically lower than those reported from fluorometric analysis [*Jacobsen and Rai*, 1990]. Fluorometric analysis does not physically separate Chl *a* from the suite of pigments present; rather, it analyzes the pigment extract as a whole. It has been shown that Chl *b* and Chl *c* can interfere with the estimation of Chl *a* [*Coveney*, 1982; *Trees et al.*, 1985; *Welschmeyer*, 1994], and HPLC analysis indicated that

Table 4. Published Regression Equations for Isoprene Versus Chl *a*

Study (Location)	Binning Criteria/Study Location	Regression Equation[a]	R^2
Ooki et al. [2015] SST bins (Pacific Ocean/Indian Ocean/ Arctic Ocean/Southern Ocean)	<3.3°C	$9.8 \times [\text{Chl } a] + 1.49 \times \text{SST} + 0.649$	0.71
	3.3–17°C	$14.3 \times [\text{Chl } a] + 2.27 \times \text{SST} + 2.83$	0.64
	17–27°C	$20.9 \times [\text{Chl } a] - 1.92 \times \text{SST} + 63.1$	0.77
	>27°C	$319 \times [\text{Chl } a] + 8.55 \times \text{SST} - 244$	0.75
Broadgate et al. [1997]	Southern Ocean and North Sea	$6.4 \times [\text{Chl } a] + 1.2$	0.62
Kurihara et al. [2010][b]	North Pacific	$18.8 \times [\text{Chl } a] + 6.1$	0.79
Kurihara et al. [2012]	Temperate Pacific (Sagami Bay)	$10.7 \times [\text{Chl } a] + 5.9$	0.49
Hashimoto et al. [2009][c]	Subarctic Pacific	$8.2 \times [\text{Chl } a] + 16$	0.67
Exton et al. [2013][d] biome (latitude) bins (laboratory; production rates)	Polar (60–90°N and 60–90°S)	$0.03(\pm0.006) \times [\text{Chl } a] + 6.20(\pm8.39) \times 10^{-7}$	0.76
	Temperate (23.5–60°N and 23.5–60°S)[e]	$0.24(\pm0.056) \times [\text{Chl } a] + 2.50(\pm4.18) \times 10^{-6}$ {$0.04(\pm0.025) \times [\text{Chl } a] + 1.50(\pm0.32) \times 10^{-5}$}	0.43 {0.08}
	Tropical (23.5°N–23.5°S)	$0.39(\pm0.221) \times [\text{Chl } a] + 1.30(\pm1.44) \times 10^{-5}$	0.15

[a] [Chl *a*] in $\mu g\ L^{-1}$.
[b] Using entire depth profiles for correlation rather than surface values only.
[c] Values given by *Kurihara et al.* [2012].
[d] (±standard error).
[e] Without outlying value, equation in curly brackets includes the outlying value.

both Chl *b* and Chl *c* were present in samples from this study. Additionally, the pigment extraction method should be considered as a source of discrepancy between the two results. While both methods used 90% acetone as a solvent, extraction for fluorometric analysis relied on this solution over time to fully extract the pigments. This has been suggested to be less efficient than additionally using physical disruption through sonication [*Neveux and Panouse*, 1987; *Jacobsen and Rai*, 1990], which was the extraction method used for HPLC analysis.

Associations of isoprene with specific pigments other than Chl *a* are consistent with the literature, as the isoprene-pigment correlations found in this study included both fucoxanthin and zeaxanthin (Figures S2–S3 in the supporting information). Diatoms, which contain fucoxanthin as a dominant carotenoid, have been shown to produce isoprene [*Moore et al.*, 1994; *Milne et al.*, 1995; *McKay et al.*, 1996; *Colomb et al.*, 2009; *Bonsang et al.*, 2010; *Exton et al.*, 2013]. *Prochlorococcus spp*. have also been shown to produce isoprene [*Shaw et al.*, 2003] and contain zeaxanthin. However, a significant correlation between isoprene and DV-Chl *a*, which is specific to *Prochlorococcus*, was only present in the high SST bin (Figure S2), so although *Prochlorococcus* may at least be partly responsible for the isoprene signal at high SST, other phytoplankton containing zeaxanthin are also likely to have contributed throughout.

3.5. Predicting Isoprene Concentrations From In Situ Observations

The regression equations (Table 3) were used to predict isoprene concentrations from the different biological measurements made during each cruise and were found to replicate the observed surface isoprene reasonably well (Figure 7; Table S2 in the supporting information). The empirical formulae published by *Ooki et al.* [2015] (referred to as O15; details in Table 4) were also applied to the current data sets and gave generally good agreement except for Arctic data and between 20 and 27°C SST (both underpredicted by O15; Figure 7).

3.6. Predicting Isoprene Concentrations From Remotely Sensed Data

Satellite data could provide a basis for global extrapolation using the empirical relationships presented here, if they can be shown to reproduce observations well. Ocean surface Chl *a* concentration is a standard satellite product, the accuracy of which has been rigorously assessed for the Atlantic Ocean [*Brewin et al.*, 2016]. IntPP has become routinely derived from remote measurements and is well validated [*Tilstone et al.*, 2009, 2015a, 2015b; *Carr et al.*, 2006; *Friedrichs et al.*, 2009; *Saba et al.*, 2010; *Brewin et al.*, 2017]. Both were used here to evaluate their suitability for predicting marine isoprene concentrations, and hence ultimately sea-to-air

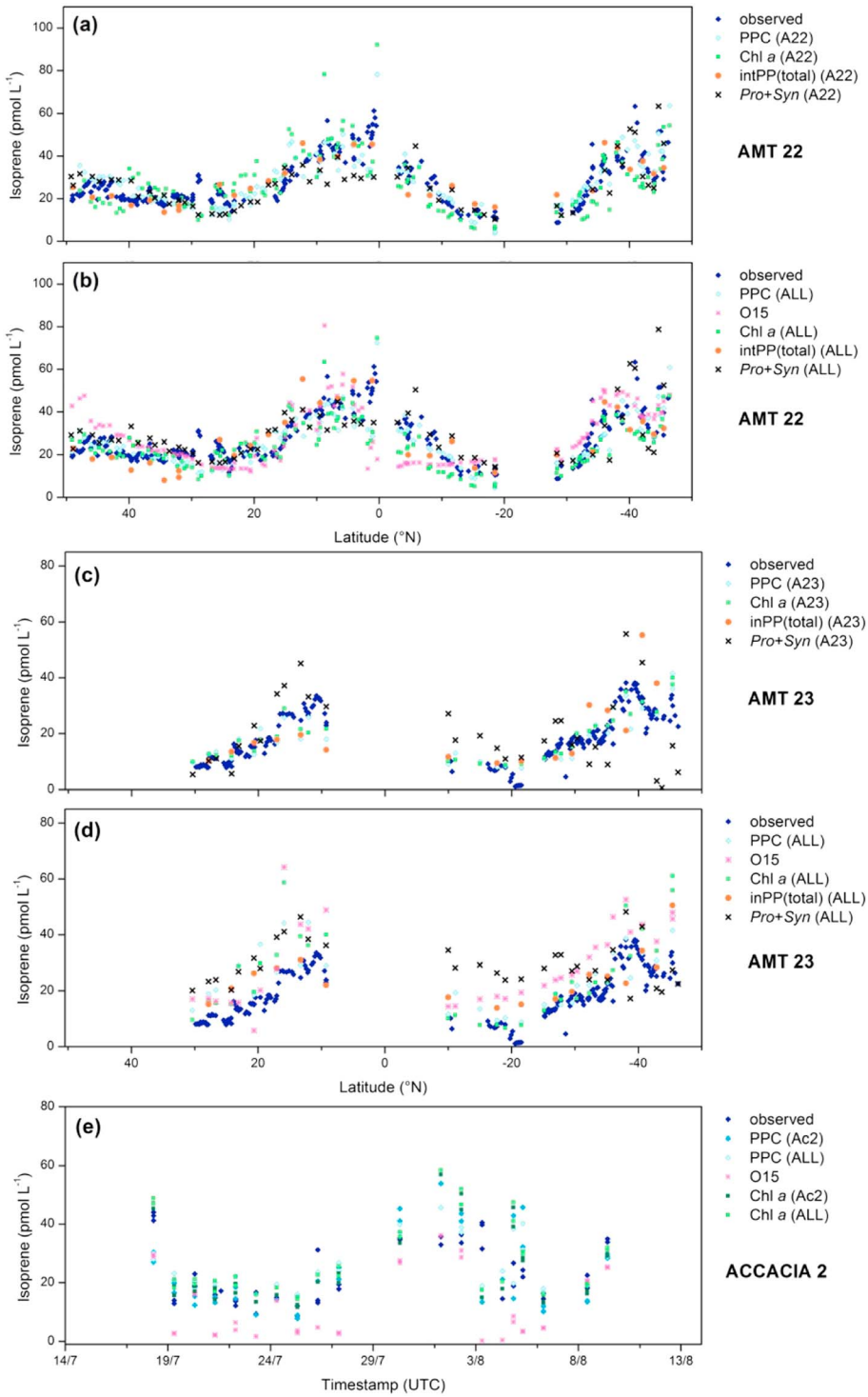

Figure 7. Observed isoprene concentrations alongside predicted values using parameterizations as shown in the legends (details see main text): relationships based on the respective data set itself (A22 and A23) and also O15 and ALL relationships for each cruise: (a) A22 and (b) O15/ALL applied to AMT 22, (c) A23 and (d) O15/ALL applied to AMT 23, and (e) Ac2 and also O15 and ALL applied to ACCACIA 2.

fluxes, globally. The best match with in situ data would be expected for daily satellite products; however, we also investigate the performance of composite images compiled over longer time periods, which are relevant for stable areas of the ocean such as Atlantic oligotrophic gyres, as daily images provide less comprehensive data due to cloud and reduced spatial coverage.

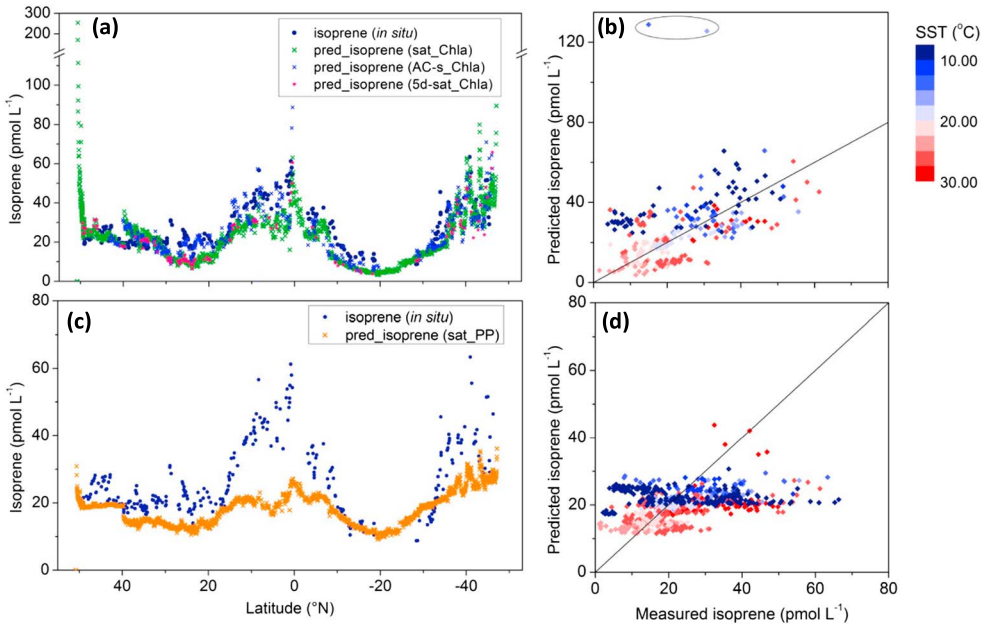

Figure 8. In situ and satellite-derived predicted isoprene concentrations from this work; (a) AMT 22, Chl-based algorithm, with satellite-derived monthly data extracted every 20 min along the cruise track and "5d"-satellite data from matchups ±2 days of the observation, alongside isoprene based on in situ AC-s [Chl *a*]; (b) all data (AMT, ACCACIA) matched with "5 day" satellite-derived data, for Chl-based algorithm, with 1:1 line; (c) as Figure 8a but for intPP-based algorithm (monthly satellite data only); (d) as Figure 8c but for monthly satellite data and intPP-based algorithm. Some outlier points (circled; coastal data) were excluded from the correlation. Further data in Figure S6 (supporting information).

Only paired values for isoprene observations and satellite-derived values were used in comparisons. Only a few pairs were available at low SST due to comparatively poor satellite coverage and increased cloud cover over high latitudes. The satellite validation was performed using the full data set, but as a control was also calculated for only independent data (Text S3.2 in the supporting information).

Predicted isoprene from optically derived in situ [Chl *a*] produced a close match with observations (Figures 8a and S6a in the supporting information), showing that the algorithm works well with underway measurements of Chl *a* derived from the absorptive properties of phytoplankton particles, which were validated and corrected for bias against HPLC pigment measurements on the same cruise [*Brewin et al*., 2016].

There was also overall good agreement between observations and isoprene estimated from both daily and monthly satellite [Chl *a*] (Figures 8a and 8b; Table S1 and Figure S6a in the supporting information), with trends being captured well for the AMT cruises and predicted values within a factor of 3 of the measurements 90% of the time. No obvious difference could be seen in goodness of fit between the daily and monthly data (Figure 8b; Figure S6b in the supporting information; $R^2 = 0.33$ and 0.23, respectively). A slight underestimation in the oligotrophic gyres (higher SST) could be partially due to degradation of the sensor (slightly lower satellite [Chl *a*] than in situ techniques in recent years) [*Brewin et al*., 2016]. For coastal data (>50°N), satellite [Chl *a*] resulted in significant overestimation (Figure 8a; Figure S6a in the supporting information), which could be related to the use of an open ocean algorithm for optically complex waters.

Overestimation of isoprene concentrations in some coastal locations can also be observed in a comparison of O15 with satellite-derived values (Figure 9a). However, the inverse is even more common for that data set: in situ data near the Japanese coast (around 138–148°E, 34–44°N; especially April/May 2009) show high isoprene concentrations of >100 pmol L^{-1} (cf. Figure 1), which are often underestimated by a factor of 2–4 by the satellite algorithm. Even though it does not capture the magnitude of the variations (Figure S8 in the supporting information), the [Chl *a*]-based algorithm is able to reproduce general trends in the in situ data and 90% of the absolute measured values within a factor of 3 (Table S2 in the supporting information).

Monthly intPP predicts isoprene with varying degrees of success: AMT data are generally good (91% within a factor of 2), with the exception of low latitudes (high SST; Figure 8c; Figure S6 in the supporting information).

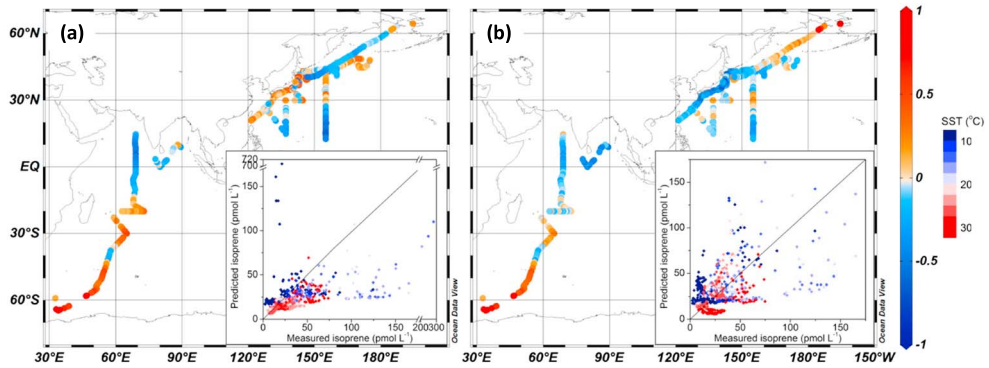

Figure 9. Ratio ($\log_{10}$ scale) of predicted isoprene from satellite data to the *Ooki et al*. [2015] data set; (a) using Chl *a*-based algorithm (one outlier at 1.5) and (b) using intPP-based algorithm (full-scale version of inset graph in supporting information Figure S7). Maps created with Ocean Data View [*Schlitzer*, 2016].

Arctic values are within a factor of 10 (96% within factor of 5) of the measurements, but trends are not always reproduced and additionally suffer from sparse coverage particularly in spring (Figure S6 in the supporting information). A comparison of intPP-predicted isoprene with O15 data appears reasonable (Figure 9b inset graph; Table S3 in the supporting information), but there is significant underprediction in the tropical North Pacific (Figure 9b). A latitudinal plot shows that performance is also poor at high latitudes and trends are not reflected very well overall (Figure S8 in the supporting information).

These difficulties can be partly attributed to the satellite product being less well validated than Chl *a*, especially outside the Atlantic, and can vary significantly depending on the satellite model used [*Carr et al*., 2006]. *Lee et al*. [2015] suggest that PP models need to be carefully tuned for the Arctic in order to perform well for that region and note that the variability of PP is underestimated by most models. Furthermore, PP measured in situ using ^{14}C on-deck incubations has been found to differ significantly from other methods [*Quay et al*., 2010]. The satellite production model used here was not parameterized using on-deck incubations, instead using photosynthesis-irradiance experiments [*Brewin et al*., 2017]. IntPP is controlled by a variety of factors; its relationship with isoprene may be less consistent on a global scale than for Chl *a*, and relationships for the open ocean cannot necessarily be applied to coastal regions. In addition, despite a similar correlation coefficient and bias for the intPP-based algorithm compared to that based on Chl *a*, the regression was performed for far fewer points and should therefore be considered less reliable. Despite these issues, the algorithm still predicts observed values within a factor of 3 for all oceanic regions evaluated here at least 84% of the time (and 98% within a factor of 5; Table S3 in the supporting information).

4. Conclusions

We found strong relationships between surface ocean isoprene concentrations and concurrently monitored biological variables such as Chl *a*, PFTs, and productivity, with better correlations for two separate SST bins with a threshold at 20°C. This is qualitatively consistent with previous studies [*Bonsang et al*., 1992; *Moore et al*., 1994; *Milne et al*., 1995; *McKay et al*., 1996; *Broadgate et al*., 1997; *Baker et al*., 2000; *Shaw et al*., 2003; *Wingenter et al*., 2004; *Moore and Wang*, 2006; *Gantt et al*., 2009; *Bonsang et al*., 2010; *Exton et al*., 2013; *Kurihara et al*., 2010, 2012; *Kameyama et al*., 2014; *Ooki et al*., 2015]. Our current lack of understanding of isoprene production processes and biological functions prevents an assignment of factors responsible for this threshold. We also observed associations of isoprene with specific pigments other than Chl *a*, which to our knowledge have not been previously reported. A strong and relatively consistent relationship with the sum of photoprotective carotenoids across all three cruises,

$$[\text{isoprene}] = 102\times[\text{PPC}] + 14.4 \left(R^2 = 0.48;\ <20°\text{C}\right) \quad (1)$$

$$[\text{isoprene}] = 345\times[\text{PPC}] - 0.81 \left(R^2 = 0.61;\ \geq 20°\text{C}\right), \quad (2)$$

could point to a photoprotective function of isoprene or at least to isoprene being a by-product of a

photoprotective response of the organisms present. An alternative explanation could be the effect of a physical driver that affects both PPC and isoprene abundances: photoprotective pigments are abundant in surface samples in highly stratified marine environments due to the high light exposure of the cells [*Babin et al*., 1996]. This could also correlate with other light-driven reactions or processes that occur under these conditions and may increase isoprene concentrations. Emission has been linked to light (and light stress) by various laboratory studies [*Shaw et al*., 2003; *Gantt et al*., 2009; *Bonsang et al*., 2010; *Meskhidze et al*., 2015] but not yet directly to a photoprotective mechanism of the phytoplankton such as has been proposed for terrestrial plants [*Sharkey and Yeh*, 2001].

Arguably, individual regression analyses have limited diagnostic potential as each assumes by definition that the investigated variable is solely responsible for the total isoprene, so that the resulting equation is only useful for predicting isoprene if that assumption is true and the variables are independent of each other. Following the same argument, a steeper slope by no means automatically implies that the entity in question (e.g., microplankton; cf. Figure S5 in the supporting information) is a strong emitter: the phenomenon can also be caused by the presence of other organisms or processes responsible for isoprene emission in regions where the examined variable has low concentrations.

For a global emission estimate, the investigated variables must have good global coverage so that an extrapolation using the equations presented here is possible. Currently, surface [Chl *a*] is available as a standard satellite product, while dominant PFTs can be obtained from ocean color satellite products using the PHYSAT method [*Alvain et al*., 2008; *Brewin et al*., 2011; *Ben Mustapha et al*., 2014; *IOCCG*, 2014] and intPP can also be derived from satellite data [*Carr et al*., 2006; *Brewin et al*., 2017]. Information on PPC distributions can be obtained from data sets such as MAREDAT [*Peloquin et al*., 2013] and, potentially, from biogeochemical and ecosystem models that are beginning to resolve PPC concentrations on regional and global scales [*Bissett et al*., 1999, *Dutkiewicz et al*., 2015]. If all parameterizations found here can be extrapolated, the degree to which they converge on a global value should give an indication of how well they reflect the actual emissions.

The extrapolations based on satellite Chl *a* and intPP performed as part of this study, using the following equations,

$$[\text{isoprene}] = 33.2\times[\text{Chl } a] + 13.7 \left(R^2 = 0.33;\ <20°\text{C}\right) \quad (3)$$

$$[\text{isoprene}] = 266\times[\text{Chl } a] - 1.68 \left(R^2 = 0.54;\ \geq 20°\text{C}\right) \quad (4)$$

$$[\text{isoprene}] = 0.017\times(\text{intPP}) + 16 \left(R^2 = 0.30;\ <20°\text{C}\right) \quad (5)$$

$$[\text{isoprene}] = 0.086\times(\text{intPP}) + 0.084 \left(R^2 = 0.67;\ \geq 20°\text{C}\right), \quad (6)$$

show that the proposed algorithms are able to reproduce in situ data reasonably well, including data sets acquired independently and in different ocean basins. Chl *a* generally captured the shape and trends of the data better than intPP but could still not closely reproduce the magnitude of the variations.

This study has contributed a large number of observations to the existing data set of marine isoprene, covering areas of the Arctic and the Atlantic Ocean at basin scale and providing representative values of isoprene in surface water for a large range of latitudes (80°N–45°S). Using a variety of supporting data, relationships with different biological variables have been confirmed and extended. When applied to the different cruises, equations derived from the combined data sets were able to predict isoprene concentrations close to the measured values, including Arctic data. However, no single variable has been identified as a more suitable proxy for predicting isoprene concentrations in water than Chl *a*, which is currently the most widely used, except perhaps integrated PP and photoprotective carotenoids (PPC). It was nevertheless shown that a separation of ocean regions by temperature ranges is crucial for most proxies in order to obtain representative predictions with empirical relationships. The uncertainty in setting global threshold values for that separation, as seen when contrasting Atlantic and Pacific/Indian Ocean data sets, highlights the need for further field measurements spanning different oceans and seasons and comparison of empirical relationships between studies. Ideally, trace gas measurements should be accompanied by as wide a range of biological measurements as possible, in order to validate the correlations found in this work and examine the suitability of the suggested additional proxies for predicting isoprene concentrations on a global scale.

Acknowledgments
This study was funded by NERC grants NE/K004980/1 and NE/K006665/1 (ORC3 project) and NE/I028769/1 (ACCA CIA project) and uses data from NMF (NERC), provided by the British Oceanographic Data Centre and funded by the Oceans 2025 program (AMT 22), and as part of NERC's National Capability program (AMT 23) and the NERC Arctic Research Programme (ACCACIA). S.H.'s PhD studentship was supported by a NERC Doctoral Training Grant (DTG) (2011–2015). R.J.W.B. and G. D. were supported by the UK National Centre for Earth Observation. G.T., R.A., and D.C. were supported by the NERC National Capability Atlantic Meridional Transect program. The authors would like to thank the personnel of the RRS *James Cook*, RRS *James Clark Ross*, and R/V *Lance*. GEOS-Chem model output was provided by T. Sherwen. Thanks also to A. Hickman for helpful discussion. Data are held at the British Oceanographic Data Centre (ACCACIA at https://www.bodc.ac.uk/resources/inventories/edmed/report/6554/; AMT 22 at https://www.bodc.ac.uk/projects/data_management/uk/amt/data_inventories/cruise/jc079/; and AMT 23 at https://www.bodc.ac.uk/projects/data_management/uk/amt/data_inventories/cruise/jr20131005/) and are available publicly or upon request. We declare no conflict of interest. This study is a contribution to the international IMBER project and was supported by the UK Natural Environment Research Council National Capability funding to Plymouth Marine Laboratory and the National Oceanography Centre, Southampton. This is contribution number 297 of the AMT program.

References

Acuña Alvarez, L., D. A. Exton, K. N. Timmis, D. J. Suggett, and T. J. McGenity (2009), Characterization of marine isoprene-degrading communities, *Environ. Microbiol.*, *11*(12), 3280–3291, doi:10.1111/j.1462-2920.2009.02069.x.

Aiken, J., Y. Pradhan, R. Barlow, S. Lavender, A. Poulton, P. Holligan, and N. Hardman-Mountford (2009), Phytoplankton pigments and functional types in the Atlantic Ocean: A decadal assessment, 1995–2005, *Deep Sea Res., Part II*, *56*(15), 899–917, doi:10.1016/j.dsr2.2008.09.017.

Andrews, S. J., S. C. Hackenberg, and L. J. Carpenter (2015), Technical Note: A fully automated purge and trap GC-MS system for quantification of volatile organic compound (VOC) fluxes between the ocean and atmosphere, *Ocean Sci.*, *11*(2), 313–321, doi:10.5194/os-11-313-2015.

Alvain, S., C. Moulin, Y. Dandonneau, and H. Loisel (2008), Seasonal distribution and succession of dominant phytoplankton groups in the global ocean: A satellite view, *Global Biogeochem. Cycles*, *22*, 1–15, doi:10.1029/2007GB003154.

Arnold, S. R., et al. (2009), Evaluation of the global oceanic isoprene source and its impacts on marine organic carbon aerosol, *Atmos. Chem. Phys.*, *9*(4), 1253–1262, doi:10.5194/acp-9-1253-2009.

Babin, M., A. Morel, H. Claustre, A. Bricaud, Z. Kolber, and P. G. Falkowski (1996), Nitrogen- and irradiance-dependent variations of the maximum quantum yield of carbon fixation in eutrophic, mesotrophic and oligotrophic marine systems, *Deep Sea Res., Part I*, *43*(8), 1241–1272, doi:10.1016/0967-0637(96)00058-1.

Baker, A. R., S. M. Turner, W. J. Broadgate, A. Thompson, G. B. McFiggans, O. Vesperini, P. D. Nightingale, P. S. Liss, and T. D. Jickells (2000), Distribution and sea-air fluxes of biogenic trace gases in the eastern Atlantic Ocean, *Global Biogeochem. Cycles*, *14*(3), 871–886, doi:10.1029/1999GB001219.

Barlow, R. G., D. G. Cummings, and S. W. Gibb (1997), Improved resolution of mono- and divinyl chlorophylls *a* and *b* and zeaxanthin and lutein in phytoplankton extracts using reverse phase C-8 HPLC, *Mar. Ecol. Prog. Ser.*, *161*, 303–307, doi:10.3354/meps161303.

Ben Mustapha, Z., S. Alvain, C. Jamet, H. Loisel, and D. Dessailly (2014), Automatic classification of water-leaving radiance anomalies from global SeaWiFS imagery: Application to the detection of phytoplankton groups in open ocean waters, *Remote Sens. Environ.*, *146*, 97–112, doi:10.1016/j.rse.2013.08.046.

Bissett, W. P., K. L. Carder, J. J. Walsh, and D. A. Dieterle (1999), Carbon cycling in the waters of the Sargasso Sea: II. Numerical simulation of apparent and inherent optical properties, *Deep Sea Res., Part I*, *46*(2), 271–317.

Bonsang, B., C. Polle, and G. Lambert (1992), Evidence for marine production of isoprene, *Geophys. Res. Lett.*, *19*(11), 1129–1132, doi:10.1029/92GL00083.

Bonsang, B., V. Gros, I. Peeken, N. Yassaa, K. Bluhm, E. Zoellner, R. Sarda-Esteve, and J. Williams (2010), Isoprene emission from phytoplankton monocultures: The relationship with chlorophyll-*a*, cell volume and carbon content, *Environ. Chem.*, *7*, 55–563, doi:10.1071/EN09156.

Brewin, R. J. W., N. J. Hardman-Mountford, S. J. Lavender, D. E. Raitsos, T. Hirata, J. Uitz, E. Devred, A. Bricaud, A. Ciotti, and B. Gentili (2011), An intercomparison of bio-optical techniques for detecting dominant phytoplankton size class from satellite remote sensing, *Remote Sens. Environ.*, *115*(2), 325–339, doi:10.1016/j.rse.2010.09.004.

Brewin, R. J. W., G. Dall'Olmo, S. Pardo, V. van Dongen-Vogels, and E. S. Boss (2016), Underway spectrophotometry along the Atlantic Meridional Transect reveals high performance in satellite chlorophyll retrievals, *Remote Sens. Environ.*, *183*, 82–97, doi:10.1016/j.rse.2016.05.005.

Brewin, R. J. W., G. Tilstone, T. Jackson, T. Cain, P. I. Miller, P. K. Lange, A. Misra, and R. Airs (2017), Modelling size-fractionated primary production in the Atlantic Ocean from remote sensing, *Prog. Oceanogr.*, doi:10.1016/j.pocean.2017.02.002, in press.

Broadgate, W. J., P. S. Liss, and S. A. Penkett (1997), Seasonal emissions of isoprene and other reactive hydrocarbon gases from the ocean, *Geophys. Res. Lett.*, *24*(21), 2675–2678, doi:10.1029/97GL02736.

Broadgate, W., G. Malin, F. C. Küpper, A. Thompson, and P. S. Liss (2004), Isoprene and other non-methane hydrocarbons from seaweeds: A source of reactive hydrocarbons to the atmosphere, *Mar. Chem.*, *88*, 61–73, doi:10.1016/j.marchem.2004.03.002.

Carlton, A. G., C. Wiedinmyer, and J. H. Kroll (2009), A review of Secondary Organic Aerosol (SOA) formation from isoprene, *Atmos. Chem. Phys.*, *9*, 4987–5005.

Carr, M.-E., et al. (2006), A comparison of global estimates of marine primary production from ocean color, *Deep Sea Res., Part II*, *53*(5–7), 741–770, doi:10.1016/j.dsr2.2006.01.028.

Ciuraru, R., L. Fine, M. Van Pinxteren, B. D'Anna, H. Herrmann, and C. George (2015), Unravelling new processes at interfaces: Photochemical isoprene production at the sea surface, *Environ. Sci. Technol.*, *49*(22), 13,199–13,205, doi:10.1021/acs.est.5b02388.

Claeys, M., et al. (2004), Formation of secondary organic aerosols through photooxidation of isoprene, *Science*, *303*(5661), 1173–1176, doi:10.1126/science.1092805.

Cohen, J., and P. Cohen (1983), Applied multiple regression/correlation analysis for the behavioral sciences, *Hillsdale, NJ Erlbaum*.

Colomb, A., V. Gros, S. Alvain, R. Sarda-Esteve, B. Bonsang, C. Moulin, T. Klüpfel, and J. Williams (2009), Variation of atmospheric volatile organic compounds over the Southern Indian Ocean (30–49°S), *Environ. Chem.*, *6*(1), 70–82, doi:10.1071/EN08072.

Coveney, M. F. (1982), Bacterial uptake of photosynthetic carbon from freshwater phytoplankton, *Oikos*, *38*(1), 8–20.

Dall'Olmo, G., E. Boss, M. J. Behrenfeld, and T. K. Westberry (2012), Particulate optical scattering coefficients along an Atlantic Meridional Transect, *Opt. Express*, *20*(19), 21,532–21,551, doi:10.1364/OE.20.021532.

de Boyer Montégut, C., G. Madec, A. S. Fischer, A. Lazar, and D. Iudicone (2004), Mixed layer depth over the global ocean: An examination of profile data and a profile-based climatology, *J. Geophys. Res.*, *109*, C12003, doi:10.1029/2004JC002378.

Dutkiewicz, S., A. E. Hickman, O. Jahn, W. W. Gregg, C. B. Mouw, and M. J. Follows (2015), Capturing optically important constituents and properties in a marine biogeochemical and ecosystem model, *Biogeosciences*, *12*(14), 4447–4481, doi:10.5194/bg-12-4447-2015.

Efron, B. (1979), Bootstrap methods: Another look at the jackknife, *Ann. Stat.*, *7*, 1–26.

Exton, D. A., D. J. Suggett, T. J. McGenity, and M. Steinke (2013), Chlorophyll-normalized isoprene production in laboratory cultures of marine microalgae and implications for global models, *Limnol. Oceanogr.*, *58*(4), 1301–1311, doi:10.4319/lo.2013.58.4.1301.

Friedrichs, M. A. M., et al. (2009), Assessing the uncertainties of model estimates of primary productivity in the tropical Pacific Ocean, *J. Mar. Syst.*, *76*(1–2), 113–133, doi:10.1016/j.jmarsys.2008.05.010.

Galbally, I. E., S. J. Lawson, I. A. Weeks, S. T. Bentley, R. W. Gillett, M. Meyer, and A. H. Goldstein (2007), Volatile organic compounds in marine air at Cape Grim, Australia, *Environ. Chem.*, *4*, 178–182, doi:10.1071/EN07024.

Gantt, B., N. Meskhidze, and D. Kamykowski (2009), A new physically-based quantification of marine isoprene and primary organic aerosol emissions, *Atmos. Chem. Phys.*, *9*(14), 4915–4927, doi:10.5194/acp-9-4915-2009.

Graff, J. R., T. K. Westberry, A. J. Milligan, M. B. Brown, G. Dall'Olmo, V. van Dongen-Vogels, K. M. Reifel, and M. J. Behrenfeld (2015), Analytical phytoplankton carbon measurements spanning diverse ecosystems, *Deep Sea Res., Part I*, *102*, 16–25, doi:10.1016/j.dsr.2015.04.006.

Guenther, A. B., X. Jiang, C. L. Heald, T. Sakulyanontvittaya, T. Duhl, L. K. Emmons, and X. Wang (2012), The Model of Emissions of Gases and Aerosols from Nature version 2.1 (MEGAN2.1): An extended and updated framework for modeling biogenic emissions, *Geosci. Model Dev.*, *5*(6), 1471–1492, doi:10.5194/gmd-5-1471-2012.

Hashimoto, S., et al. (2009), Production and air-sea flux of halomethanes in the western subarctic Pacific in relation to phytoplankton pigment concentrations during the iron fertilization experiment (SEEDS II), *Deep. Res., Part II*, *56*(26), 2928–2935, doi:10.1016/j.dsr2.2009.07.003.

Heywood, J. L., M. V. Zubkov, G. A. Tarran, B. M. Fuchs, and P. M. Holligan (2006), Prokaryoplankton standing stocks in oligotrophic gyre and equatorial provinces of the Atlantic Ocean: Evaluation of inter-annual variability, *Deep Sea Res., Part II*, *53*(14–16), 1530–1547, doi:10.1016/j.dsr2.2006.05.005.

Holm-Hansen, O., C. J. Lorenzen, R. W. Holmes, and J. D. H. Strickland (1965), Fluorometric determination of chlorophyll, *ICES J. Mar. Sci.*, *30*(1), 3–15, doi:10.1093/icesjms/30.1.3.

Hooker, S. B., et al. (2005), The Second SeaWiFS HPLC Analysis Round-Robin experiment (SeaHARRE-2), NASA Tech. Memo,Goddard Sp. Flight Cent., 2005–21278 (August), 112 pp.

Hopkins, J. R., I. D. Jones, A. C. Lewis, J. B. McQuaid, and P. W. Seakins (2002), Non-methane hydrocarbons in the Arctic boundary layer, *Atmos. Environ.*, *36*(20), 3217–3229, doi:10.1016/S1352-2310(02)00324-2.

Hopkins, J. R., C. E. Jones, and A. C. Lewis (2011), A dual channel gas chromatograph for atmospheric analysis of volatile organic compounds including oxygenated and monoterpene compounds, *J. Environ. Monit.*, 2268–2276, doi:10.1039/c1em10050e.

IOCCG (2014), Phytoplankton Functional Types from Space, edited by S. Sathyendranath, Reports of the International Ocean-Colour Coordinating Group, No. 15, IOCCG, Dartmouth, Canada.

Ito, A., and M. Kawamiya (2010), Potential impact of ocean ecosystem changes due to global warming on marine organic carbon aerosols, *Global Biogeochem. Cycles*, *24*, GB1012, doi:10.1029/2009GB003559.

Jackson, T. (2013), *Phytoplankton Community Structure, Photophysiology and Primary Production in the Atlantic Arctic*, Univ. of Oxford, Oxford, U. K.

Jacobsen, T. R., and H. Rai (1990), Comparison of spectrophotometric, fluorometric and high performance liquid chromatography methods for determination of chlorophyll *a* in aquatic samples: Effects of solvent and extraction procedures, *Int. Rev. Gesamten Hydrobiol. Hydrogr.*, *75*(2), 207–217, doi:10.1002/iroh.19900750207.

Johnson, M. T. (2010), A numerical scheme to calculate temperature and salinity dependent air-water transfer velocities for any gas, *Ocean Sci.*, *6*(4), 913–932, doi:10.5194/os-6-913-2010.

Kameyama, S., H. Tanimoto, S. Inomata, U. Tsunogai, A. Ooki, S. Takeda, H. Obata, A. Tsuda, and M. Uematsu (2010), High-resolution measurement of multiple volatile organic compounds dissolved in seawater using equilibrator inlet–proton transfer reaction-mass spectrometry (EI–PTR-MS), *Mar. Chem.*, *122*(1–4), 59–73, doi:10.1016/j.marchem.2010.08.003.

Kameyama, S., S. Yoshida, H. Tanimoto, S. Inomata, K. Suzuki, and H. Yoshikawa-Inoue (2014), High-resolution observations of dissolved isoprene in surface seawater in the Southern Ocean during austral summer 2010–2011, *J. Oceanogr.*, *70*(3), 225–239, doi:10.1007/s10872-014-0226-8.

Khalil, B., and J. Adamowski (2012), Record extension for short-gauged water quality parameters using a newly proposed robust version of the Line of Organic Correlation technique, *Hydrol. Earth Syst. Sci.*, *16*(7), 2253–2266, doi:10.5194/hess-16-2253-2012.

Kurihara, M. K., et al. (2010), Distributions of short-lived iodocarbons and biogenic trace gases in the open ocean and atmosphere in the western North Pacific, *Mar. Chem.*, *118*(3–4), 156–170, doi:10.1016/j.marchem.2009.12.001.

Kurihara, M., M. Iseda, T. Ioriya, N. Horimoto, J. Kanda, T. Ishimaru, Y. Yamaguchi, and S. Hashimoto (2012), Brominated methane compounds and isoprene in surface seawater of Sagami Bay: Concentrations, fluxes, and relationships with phytoplankton assemblages, *Mar. Chem.*, *134–135*, 71–79, doi:10.1016/j.marchem.2012.04.001.

Lawson, S. J., I. Galbally, E. Dunne, and J. Gras (2011), Measurement of VOCs in marine air at Cape Grim using Proton Transfer Reaction-Mass Spectrometry (PTR-MS), in *Baseline Atmospheric Program (Australia) 2007–2008—Cape Grim*, edited by N. Derek and P. B. Krummel, pp. 23–32, Australian Bureau of Meteorology and CSIRO Marine and Atmospheric Research, Melbourne.

Lawson, S. J., P. W. Selleck, I. E. Galbally, M. D. Keywood, M. J. Harvey, C. Lerot, D. Helmig, and Z. Ristovski (2015), Seasonal in situ observations of glyoxal and methylglyoxal over the temperate oceans of the Southern Hemisphere, *Atmos. Chem. Phys.*, *15*(1), 223–240, doi:10.5194/acp-15-223-2015.

Lee, Y. J., P. A. Matrai, M. A. M. Friedrichs, V. S. Saba, M. Ardyna, I. Asanuma, M. Babin, and S. Bélanger (2015), An assessment of phytoplankton primary productivity in the Arctic Ocean from satellite ocean color/in situ chlorophyll-*a* based models, *J. Geophys. Res. Oceans*, *120*, 6508–6541, doi:10.1002/2015JC011018.

Lewis, A. C., K. D. Bartle, D. E. Heard, J. B. McQuaid, M. J. Pilling, and P. W. Seakins (1997), In situ, gas chromatographic measurements of non-methane hydrocarbons and dimethyl sulfide at a remote coastal location (Mace Head, Eire) July–August 1996, *J. Chem. Soc., Faraday Trans.*, *93*, 2921–2927, doi:10.1039/A701566F.

Lewis, A. C., J. B. McQuaid, N. Carslaw, and M. J. Pilling (1999), Diurnal cycles of short-lived tropospheric alkenes at a North Atlantic coastal site, *Atmos. Environ.*, *33*(15), 2417–2422, doi:10.1016/S1352-2310(98)00429-4.

Lewis, A. C., L. J. Carpenter, and M. J. Pilling (2001), Nonmethane hydrocarbons in Southern Ocean boundary layer air, *J. Geophys. Res.*, *106*(D5), 4987–4994, doi:10.1029/2000JD900634.

Liss, P. S., and L. Merlivat (1986), Air-sea gas exchange rates: Introduction and synthesis, in *The Role of Air-Sea Exchange in Geochemical Cycling*, edited by P. Buat-Ménard, pp. 113–127, Springer, New York.

Luo, G., and F. Yu (2010), A numerical evaluation of global oceanic emissions of α-pinene and isoprene, *Atmos. Chem. Phys.*, *10*, 2007–2015.

McKay, W. A., M. F. Turner, B. M. R. Jones, and C. M. Halliwell (1996), Emissions of hydrocarbons from marine phytoplankton - some results from controlled laboratory experiments, *Atmos. Environ.*, *30*(14), 2583–2593.

Matsunaga, S., M. Mochida, T. Saito, and K. Kawamura (2002), In situ measurement of isoprene in the marine air and surface seawater from the western North Pacific, *Atmos. Environ.*, *36*, 6051–6057.

Meskhidze, N., and A. Nenes (2006), Phytoplankton and cloudiness in the Southern Ocean, *Science*, *314*(5804), 1419–23, doi:10.1126/science.1131779.

Meskhidze, N., A. Sabolis, R. Reed, and D. Kamykowski (2015), Quantifying environmental stress-induced emissions of algal isoprene and monoterpenes using laboratory measurements, *Biogeosciences*, *12*(3), 637–651, doi:10.5194/bg-12-637-2015.

Metzger, A., et al. (2010), Evidence for the role of organics in aerosol particle formation under atmospheric conditions, *Proc. Natl. Acad. Sci. U.S.A.*, *107*(15), 6646–6651, doi:10.1073/pnas.0911330107.

Milne, P. J., D. D. Riemer, R. G. Zika, and L. E. Brand (1995), Measurement of vertical distribution of isoprene in surface seawater, its chemical fate, and its emission from several phytoplankton monocultures, *Mar. Chem.*, *48*(3–4), 237–244, doi:10.1016/0304-4203(94)00059-M.

Monroe, B. M. (1981), Rate constant for the reaction of singlet oxygen with conjugated dienes, *J. Am. Chem. Soc.*, *103*, 7253–7256.

Moore, R. M., and L. Wang (2006), The influence of iron fertilization on the fluxes of methyl halides and isoprene from ocean to atmosphere in the SERIES experiment, *Deep Sea Res., Part II*, *53*(20–22), 2398–2409, doi:10.1016/j.dsr2.2006.05.025.

Moore, R. M., D. E. Oram, and S. A. Penkett (1994), Production of isoprene by marine phytoplankton cultures, *Geophys. Res. Lett.*, *21*(23), 2507–2510, doi:10.1029/94GL02363.

Neveux, J., and M. Panouse (1987), Spectrofluorometric determination of chlorophylls and pheophytins, *Arch. Hydrobiol.*, *109*(4), 567–581.

Nightingale, P. D., G. Malin, C. S. Law, A. J. Watson, P. S. Liss, M. I. Liddicoat, J. Boutin, and R. C. Upstill-Goddard (2000), In situ evaluation of air-sea gas exchange parameterizations using novel conservative and volatile tracers, *Global Biogeochem. Cycles*, *14*(1), 373–387, doi:10.1029/1999GB900091.

Ooki, A., D. Nomura, S. Nishino, T. Kikuchi, and Y. Yokouchi (2015), A global-scale map of isoprene and volatile organic iodine in surface seawater of the Arctic, Northwest Pacific, Indian, and Southern Oceans, *J. Geophys. Res. Oceans*, *120*, 4108–4128, doi:10.1002/2014JC010519.

Palmer, P. I., and S. L. Shaw (2005), Quantifying global marine isoprene fluxes using MODIS chlorophyll observations, *Geophys. Res. Lett.*, L09805, doi:10.1029/2005GL022592.

Peloquin, J., et al. (2013), The MAREDAT global database of high performance liquid chromatography marine pigment measurements, *Earth Syst. Sci. Data*, *5*(1), 109–123, doi:10.5194/essd-5-109-2013.

Quay, P. D., C. Peacock, K. Björkman, and D. M. Karl (2010), Measuring primary production rates in the ocean: Enigmatic results between incubation and non-incubation methods at Station ALOHA, *Global Biogeochem. Cycles*, *24*, GB3014, doi:10.1029/2009GB003665.

Robinson, C., P. Serret, G. Tilstone, E. Teira, M. V. Zubkov, A. P. Rees, and E. M. S. Woodward (2002), Plankton respiration in the eastern Atlantic Ocean, *Deep Sea Res., Part I*, *49*(5), 787–813, doi:10.1016/S0967-0637(01)00083-8.

Saba, V. S., et al. (2010), Challenges of modeling depth-integrated marine primary productivity over multiple decades: A case study at BATS and HOT, *Global Biogeochem. Cycles*, *24*, GB3020, doi:10.1029/2009GB003655.

Schlitzer, R. (2016), Ocean Data View. [Available at http://odv.awi.de.]

Shaw, S. L. (2001), The production of non-methane hydrocarbons by marine plankton, PhD thesis, MIT Cent. for Global Change Sci. Rep. 66, Cambridge, Mass.

Shaw, S. L., S. W. Chisholm, and R. G. Prinn (2003), Isoprene production by *Prochlorococcus*, a marine cyanobacterium, and other phytoplankton, *Mar. Chem.*, *80*(4), 227–245, doi:10.1016/S0304-4203(02)00101-9.

Shaw, S. L., B. Gantt, and N. Meskhidze (2010), Production and emissions of marine isoprene and monoterpenes: A review, *Adv. Meteorol.*, *2010*(1), 1–24, doi:10.1155/2010/408696.

Sharkey, T. D., and S. Yeh (2001), Isoprene Emission from Plants, *Annu. Rev. Plant Physiol. Plant Mol. Biol.*, *52*, 407–36.

Sherwen, T., et al. (2016), Iodine's impact on tropospheric oxidants: A global model study in GEOS-Chem, *Atmos. Chem. Phys.*, *16*(2), 1161–1186, doi:10.5194/acp-16-1161-2016.

Sinha, V., J. Williams, M. Meyerhöfer, U. Riebesell, A. I. Paulino, and A. Larsen (2007), Air-sea fluxes of methanol, acetone, acetaldehyde, isoprene and DMS from a Norwegian fjord following a phytoplankton bloom in a mesocosm experiment, *Atmos. Chem. Phys.*, *7*(3), 739–755, doi:10.5194/acp-7-739-2007.

Tarran, G. A., J. L. Heywood, and M. V. Zubkov (2006), Latitudinal changes in the standing stocks of nano- and picoeukaryotic phytoplankton in the Atlantic Ocean, *Deep Sea Res., Part II*, *53*(14–16), 1516–1529, doi:10.1016/j.dsr2.2006.05.004.

Tilstone, G. H., B. H. Taylor, D. Blondeau-Patissier, T. Powell, S. B. Groom, A. P. Rees, and M. I. Lucas (2015a), Comparison of new and primary production models using SeaWiFS data in contrasting hydrographic zones of the northern North Atlantic, *Remote Sens. Environ.*, *156*, 473–489, doi:10.1016/j.rse.2014.10.013.

Tilstone, G. H., Y. Xie, C. Robinson, P. Serret, D. E. Raitsos, T. Powell, M. Aranguren-Gassis, E. E. Garcia-Martin, and V. Kitidis (2015b), Satellite estimates of net community production indicate predominance of net autotrophy in the Atlantic Ocean, *Remote Sens. Environ.*, *164*, 254–269, doi:10.1016/j.rse.2015.03.017.

Tilstone, G., T. Smyth, A. Poulton, and R. Hutson (2009), Measured and remotely sensed estimates of primary production in the Atlantic Ocean from 1998 to 2005, *Deep Sea Res., Part II*, *56*(15), 918–930, doi:10.1016/j.dsr2.2008.10.034.

Tran, S., B. Bonsang, V. Gros, I. Peeken, R. Sarda-Esteve, A. Bernhardt, and S. Belviso (2013), A survey of carbon monoxide and non-methane hydrocarbons in the Arctic Ocean during summer 2010, *Biogeosciences*, *10*(3), 1909–1935, doi:10.5194/bg-10-1909-2013.

Trees, C. C., M. C. Kennicutt, and J. M. Brooks (1985), Errors associated with the standard fluorimetric determination of chlorophylls and phaeopigments, *Mar. Chem.*, *17*(1), 1–12, doi:10.1016/0304-4203(85)90032-5.

van Heukelem, L., and S. B. Hooker (2011), The importance of a quality assurance plan for method validation and minimizing uncertainties in the HPLC analysis of phytoplankton pigments, in *Phytoplankton Pigments*, edited by S. Roy et al., pp. 195–256, Cambridge Univ. Press, Cambridge.

Vickers, D., and L. Mahrt (1997), Quality control and flux sampling problems for tower and aircraft data, *J. Atmos. Oceanic Technol.*, *14*(3), 512–526, doi:10.1175/1520-0426(1997)014<0512:QCAFSP>2.0.CO;2.

Wanninkhof, R. (1992), Relationship between wind speed and gas exchange, *J. Geophys. Res.*, *97*(92), 7373–7382, doi:10.1029/92JC00188.

Welschmeyer, N. A. (1994), Fluorometric analysis of chlorophyll *a* in the presence of chlorophyll *b* and pheopigments, *Limnol. Oceanogr.*, *39*(8), 1985–1992, doi:10.4319/lo.1994.39.8.1985.

Williams, J., et al. (2010), Assessing the effect of marine isoprene and ship emissions on ozone, using modelling and measurements from the South Atlantic Ocean, *Environ. Chem.*, *7*(2), 171, doi:10.1071/EN09154.

Wingenter, O. W., K. B. Haase, P. Strutton, G. Friederich, S. Meinardi, D. R. Blake, and F. S. Rowland (2004), Changing concentrations of CO, CH_4, C_5H_8, CH_3Br, CH_3I, and dimethyl sulfide during the Southern Ocean Iron Enrichment Experiments, *Proc. Natl. Acad. Sci. U.S.A.*, *101*(23), 8537–8541, doi:10.1073/pnas.0402744101.

Wingenter, O. W., N. Meskhidze, and A. Nenes (2007), Isoprene, cloud droplets, and phytoplankton, *Science*, *317*(5834), 42–43, doi:10.1126/science.317.5834.42b.

Yassaa, N., I. Peeken, E. Zöllner, K. Bluhm, S. Arnold, D. V. Spracklen, and J. Williams (2008), Evidence for marine production of monoterpenes, *Environ. Chem.*, *5*(6), 391–401, doi:10.1071/EN08047.

Yokouchi, Y., H. Li, and T. Machida (1999), Isoprene in the marine boundary layer (Southeast Asian Sea, eastern Indian Ocean, and Southern Ocean): Comparison with dimethyl sulfide and bromoform, *J. Geophys. Res.*, *104*(D7), 8067–8076, doi:10.1029/1998JD100013.

Zapata, M., F. Rodríguez, and J. L. Garrido (2000), Separation of chlorophylls and carotenoids from marine phytoplankton: A new HPLC method using a reversed phase C8 column and pyridine-containing mobile phases, *Mar. Ecol. Prog. Ser.*, *195*, 29–45, doi:10.3354/meps195029.

Zindler, C., C. A. Marandino, H. W. Bange, F. Schütte, and E. S. Saltzman (2014), Nutrient availability determines dimethyl sulfide and isoprene distribution in the eastern Atlantic Ocean, *Geophys. Res. Lett.*, *41*, 3181–3188, doi:10.1002/2014GL059547.